Progress on the Development of Efficient Methods for Computational Aeroelasticity and Aerodynamic Design Optimization

Kivanc Ekici, PhD

Professor

Associate Department Head

Graduate Program Director

Mechanical, Aerospace, and Biomedical Engineering Department

University of Tennessee, Knoxville

Knoxville, TN, USA

COMPUTATIONAL FLUID DYNAMICS
LABORATORY

THE UNIVERSITY OF TENNESSEE KNOXVILLE

Acknowledgments

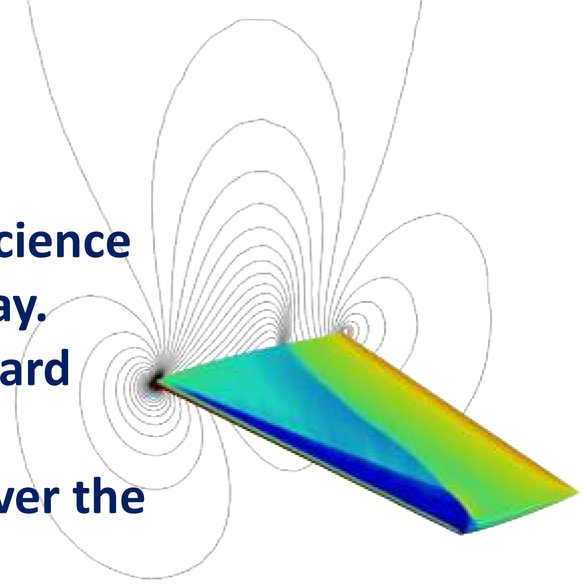

- Many thanks to our sponsors; including the National Science Foundation for its support for our work presented today.
- This work would not have been possible without the hard work and countless hours of research/code-development/debugging of our team over the years.
  - Dr. Reza Djeddi (UTK, Postdoc)
  - Dr. Hang Li (Duke U., Postdoc)
  - Mr. Andrew Kaminsky (CFDRC, finishing PhD, Senior Research Scientist)
  - Dr. Jason Howison (The Citadel, Assoc. Prof.)
  - Dr. Huang Huang (Northwestern Poly. U., Assoc. Prof.)
  - Dr. Emily Buckman (Raytheon Missile Sys, Senior Eng.
  - Dr. Franklin Curtis (Oak Ridge National Lab, Senior Res
  - Mr. Ali Nejad (NCSU-Havelock, finishing PhD, Lecturer
  - Mr. Matthew Whisenant (PhD student)
  - Mr. John Thress (PhD student)
  - Mr. Coleman Floyd (PhD student)

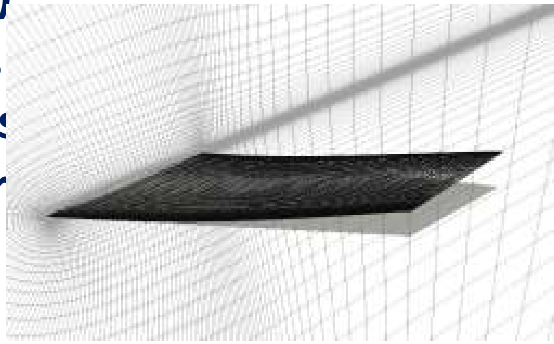

Contents

1) Flutter and LCO Predictions
   Using our State-of-the-Art "One Shot" Method

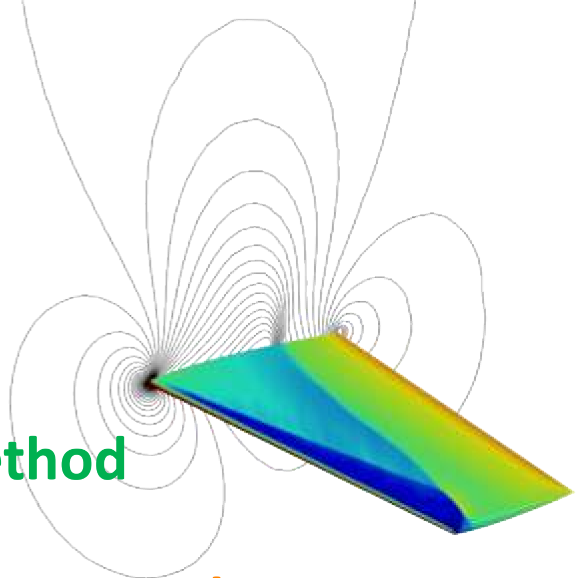

2) Adjoint-Based Sensitivity Analysis Using our Novel FDOT
   Automatic Differentiation Tool for Aerodynamic Design
   Optimization

3) Machine Learning and Artificial Neural Networks
   for Unsteady Flow Prediction

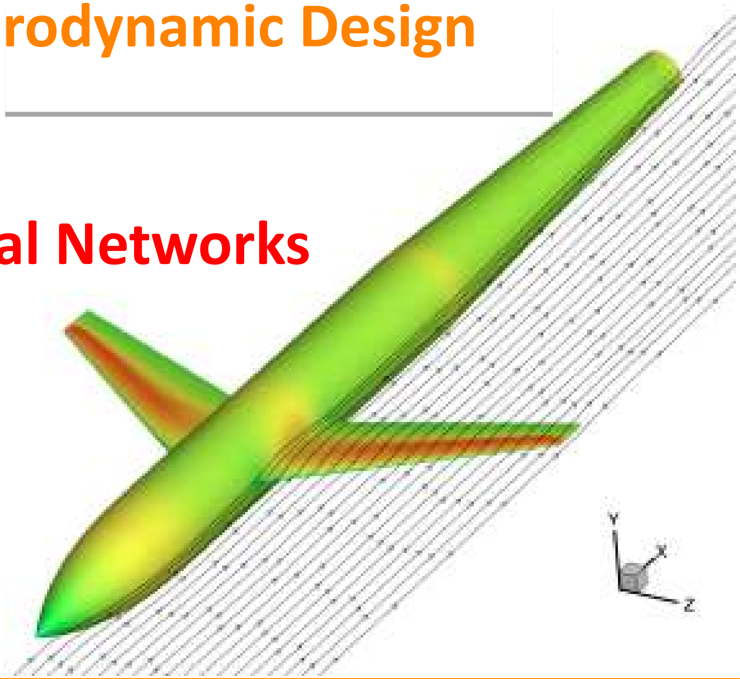

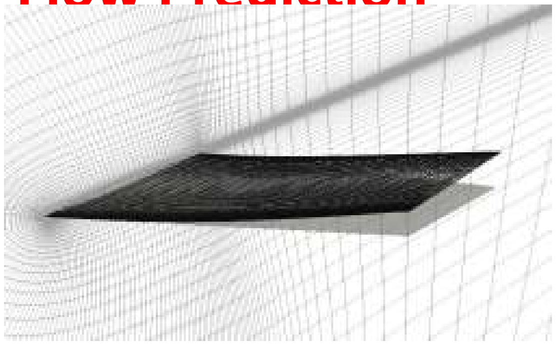

4) Conclusion

Computational Aeroelasticity using the One-Shot Method

Introduction

COMPUTATIONAL FLUID DYNAMICS
LABORATORY

THE UNIVERSITY OF
TENNESSEE
KNOXVILLE

Computational Aeroelasticity

The Collapse of Tacoma Narrows Bridge (Nov. 7th, 1940)

Transverse mode excitation followed by a torsional mode vibration caused the failure.

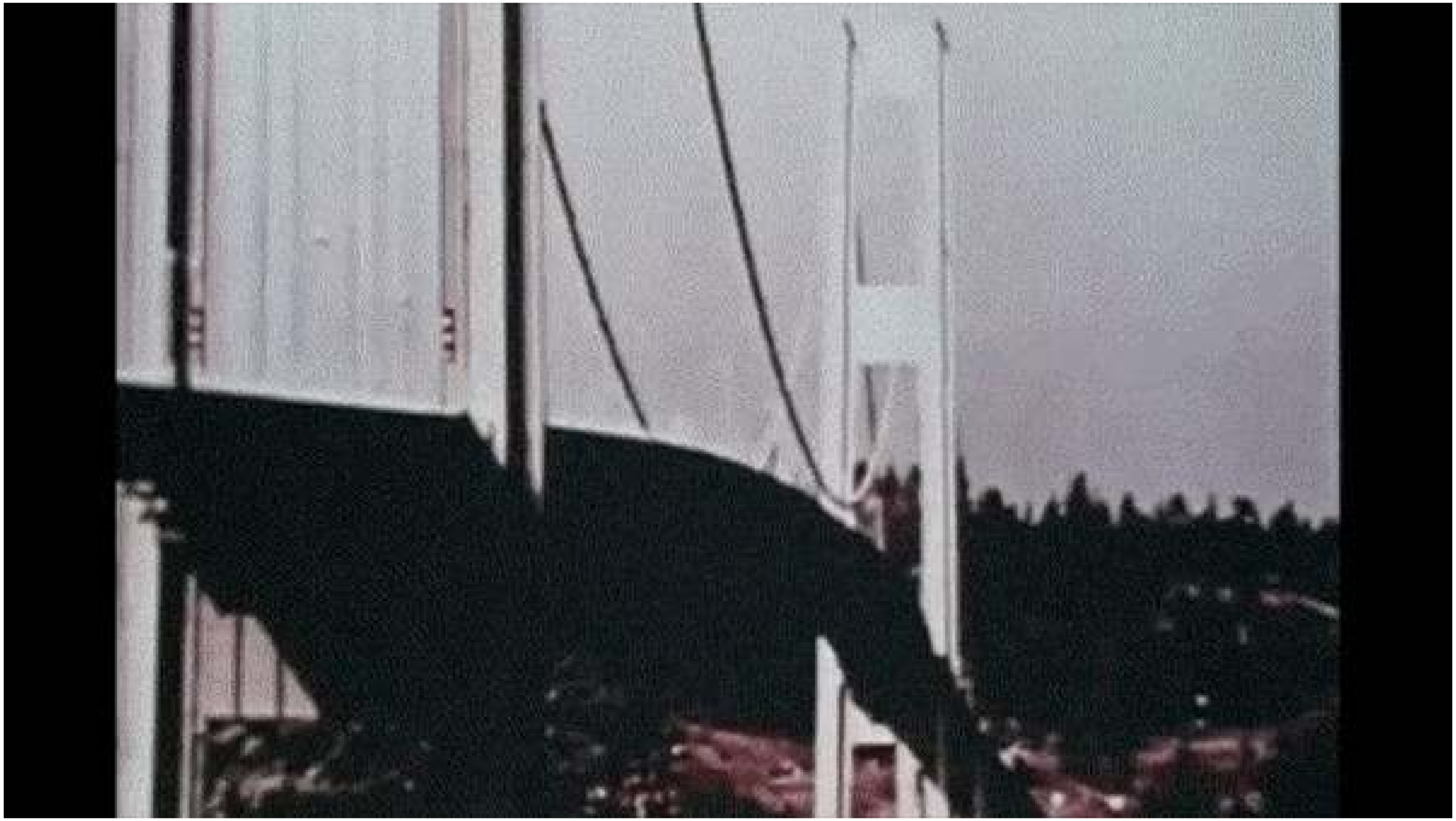

Computational Aeroelasticity

The Collar's Aeroelasticity Triangle

Collar (1946)

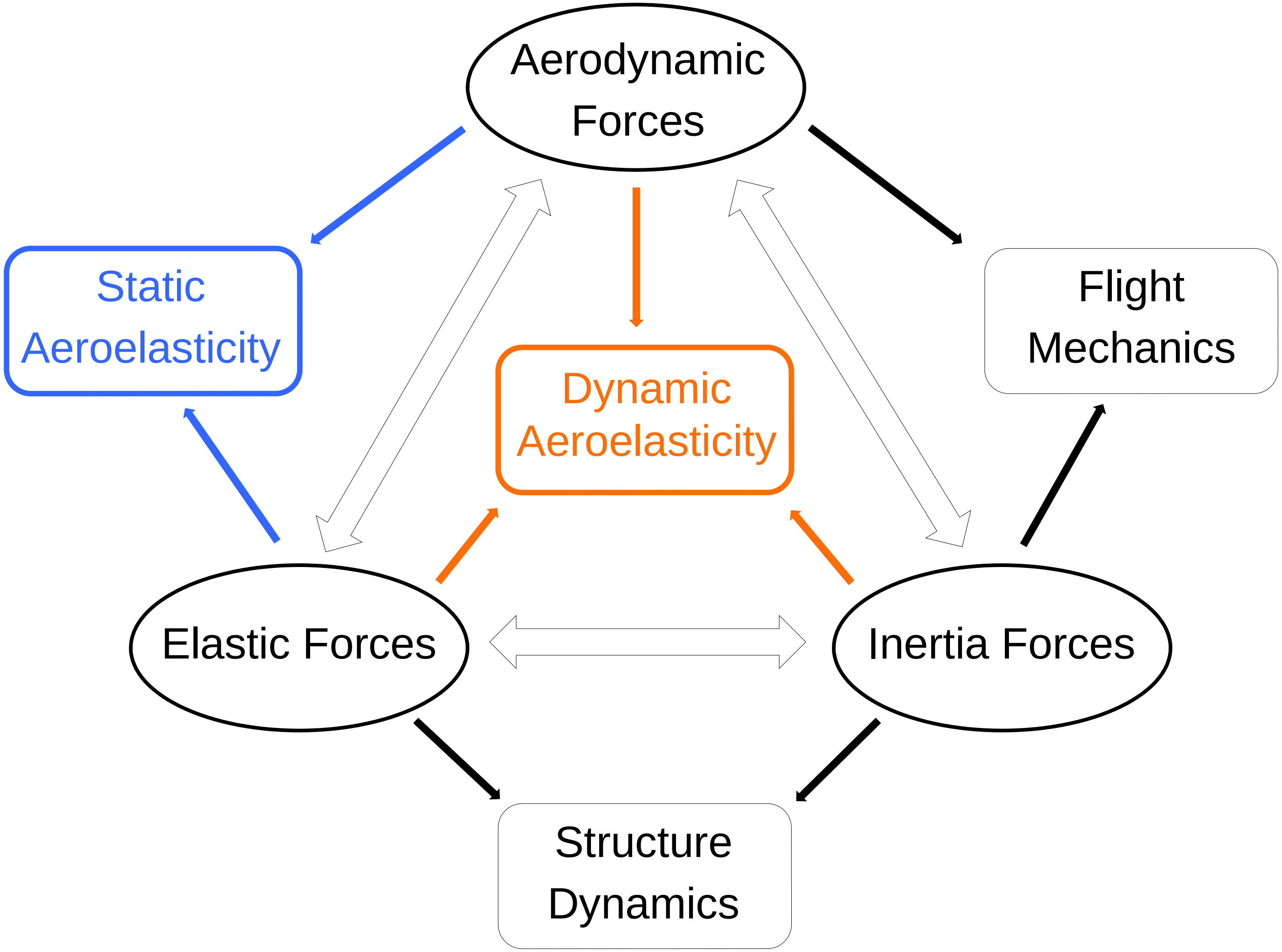

THE UNIVERSITY OF TENNESSEE KNOXVILLE

Flutter and Limit Cycle Oscillation

- **Flutter:**
  The onset point of self-excited vibration
  (Stability problem)

- **Limit Cycle Oscillation (LCO) :**
  The vibration following the flutter point having a finite amplitude
  (Response problem)

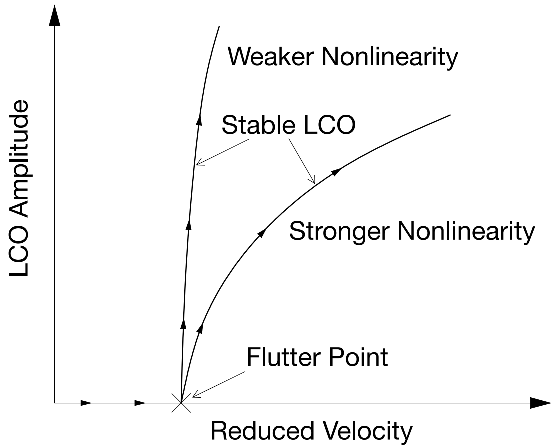

Benign LCO response

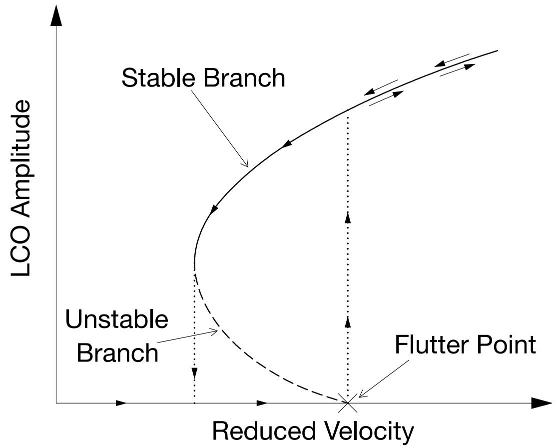

Explosive LCO response

Flutter test of the DG-300 Glider

Aeroelastic Governing Equations

- **Structure Dynamics:**

$$\boldsymbol{M}\ddot{\boldsymbol{q}} + \boldsymbol{T}\dot{\boldsymbol{q}} + \boldsymbol{K}\boldsymbol{q} = \boldsymbol{P}(\boldsymbol{q}, t)$$

- **Fluid Dynamics:** **Reynolds-Averaged Navier-Stokes (RANS) equations closed by the one equation Spalart-Allmaras turbulence model**

$$\frac{\partial \boldsymbol{U}}{\partial t} + \frac{\partial \boldsymbol{F}}{\partial x} + \frac{\partial \boldsymbol{G}}{\partial y} + \frac{\partial \boldsymbol{H}}{\partial z} = \boldsymbol{S}$$

$$\boldsymbol{U} = \begin{bmatrix} \rho \\ \rho u \\ \rho v \\ \rho w \\ \rho E \\ \rho\tilde{\nu} \end{bmatrix}, \quad \boldsymbol{F} = \begin{bmatrix} \rho u - \rho\dot{f} \\ \rho u^2 + p - \tau_{xx} - \rho u\dot{f} \\ \rho uv - \tau_{xy} - \rho v\dot{f} \\ \rho uw - \tau_{xz} - \rho w\dot{f} \\ \rho uH - \tau_{xh} - \rho E\dot{f} \\ \rho u\tilde{\nu} - \tau_{x\nu} - \rho\tilde{\nu}\dot{f} \end{bmatrix}, \quad \boldsymbol{G} = \begin{bmatrix} \rho v - \rho\dot{g} \\ \rho uv - \tau_{yx} - \rho u\dot{g} \\ \rho v^2 + p - \tau_{yy} - \rho v\dot{g} \\ \rho vw - \tau_{yz} - \rho w\dot{g} \\ \rho vH - \tau_{yh} - \rho E\dot{g} \\ \rho v\tilde{\nu} - \tau_{y\nu} - \rho\tilde{\nu}\dot{g} \end{bmatrix}, \quad \boldsymbol{H} = \begin{bmatrix} \rho w - \rho\dot{h} \\ \rho uw - \tau_{zx} - \rho u\dot{h} \\ \rho vw - \tau_{zy} - \rho v\dot{h} \\ \rho w^2 + p - \tau_{zz} - \rho w\dot{h} \\ \rho wH - \tau_{zh} - \rho E\dot{h} \\ \rho w\tilde{\nu} - \tau_{z\nu} - \rho\tilde{\nu}\dot{h} \end{bmatrix}, \quad \boldsymbol{S} = \begin{bmatrix} 0 \\ 0 \\ 0 \\ 0 \\ 0 \\ S_t \end{bmatrix}$$

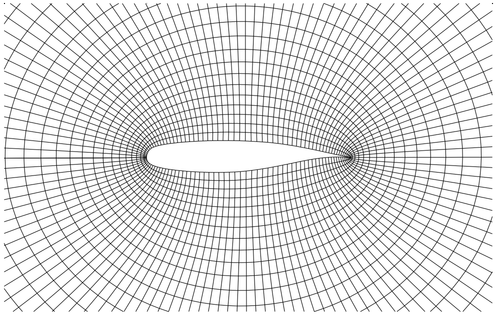

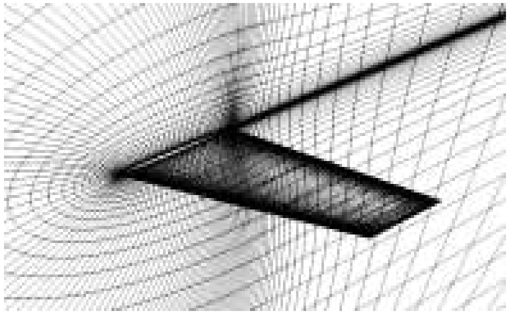

Huang and Ekici (2013), Howison and Ekici (2014)

Harmonic Balance (HB) Method

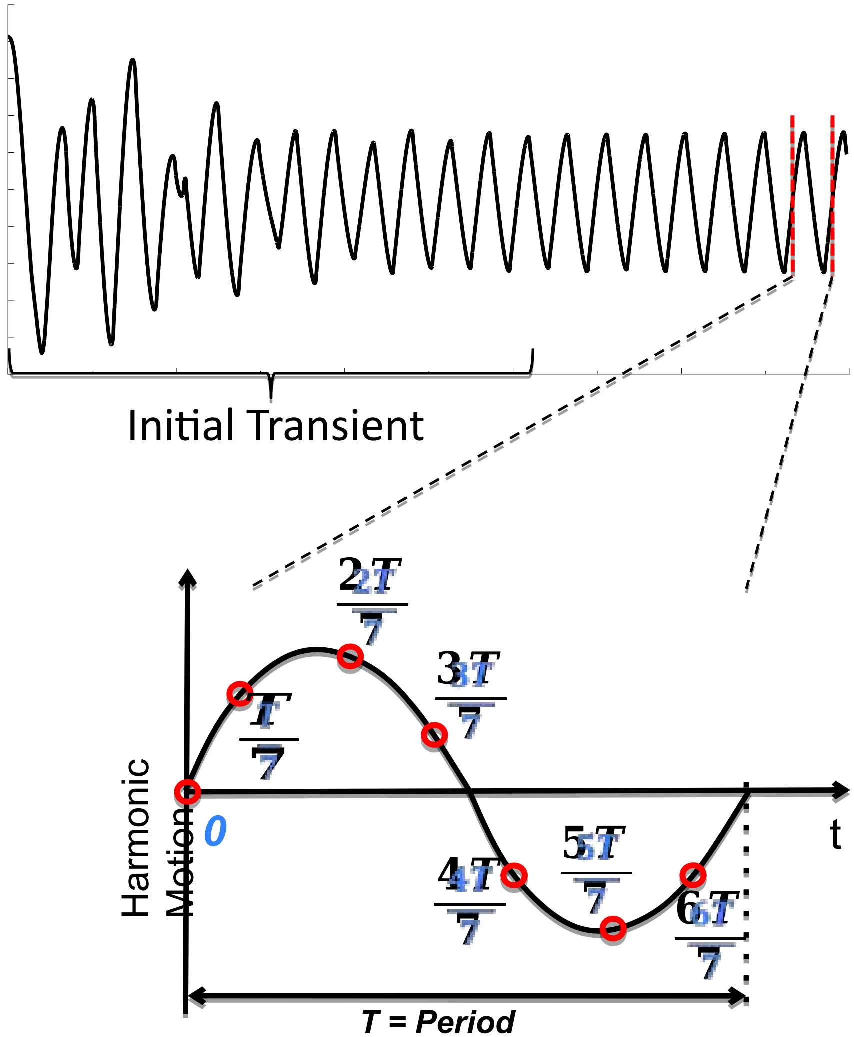

- ✓ Fourier-based mixed time-frequency domain method
- ✓ Capacity of modeling strong nonlinear periodic unsteady flows and structural vibrations by incorporating multiple harmonics
- ✓ Significant computational cost savings by transferring unsteady problem into mathematically stable problem
- ✓ More convenient to analyze the flutter and LCO problems

Hall et al. (2002, 2013) , Ekici and Huang (2012)

Harmonic Balance (HB) Method

Original RANS equation:

$$\frac{\partial \boldsymbol{U}}{\partial t}+\frac{\partial \boldsymbol{F}}{\partial x}+\frac{\partial \boldsymbol{G}}{\partial y}+\frac{\partial \boldsymbol{H}}{\partial z}=\boldsymbol{S}$$

$$\boldsymbol{U}^*=\boldsymbol{U}(x,y,t_i)=\sum_{n=0}^{N}\hat{\boldsymbol{U}}_{\boldsymbol{C}n}(x,y)\cos(\omega n t_i)+\hat{\boldsymbol{U}}_{\boldsymbol{S}n}(x,y)\sin(\omega n t_i)$$

$$\boldsymbol{U}^*=\boldsymbol{E}^{-1}\hat{\boldsymbol{U}} \Longleftrightarrow \hat{\boldsymbol{U}}=\boldsymbol{E}\boldsymbol{U}^*$$

Equation in a number of sub-time levels:

$$\frac{\partial \boldsymbol{U}^*}{\partial t}+\frac{\partial \boldsymbol{F}^*}{\partial x}+\frac{\partial \boldsymbol{G}^*}{\partial y}+\frac{\partial \boldsymbol{H}^*}{\partial z}=\boldsymbol{S}^*$$

$$\underbrace{\begin{Bmatrix}\boldsymbol{U}_1\\ \boldsymbol{U}_2\\ \boldsymbol{U}_3\\ \vdots\\ \boldsymbol{U}_{2N+1}\end{Bmatrix}}_{\boldsymbol{U}^*}$$

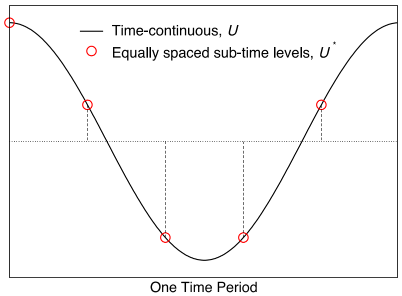

Approximate time derivative by pseudo-spectral operator:

$$\tilde{\omega}\boldsymbol{D}\boldsymbol{U}^*+\frac{\partial \boldsymbol{F}^*}{\partial x}+\frac{\partial \boldsymbol{G}^*}{\partial y}+\frac{\partial \boldsymbol{H}^*}{\partial z}=\boldsymbol{S}^* \quad \text{with} \quad \tilde{\omega}\boldsymbol{D}=\frac{d\boldsymbol{E}^{-1}}{dt}\boldsymbol{E}$$

pseudo-spectral operator

Equation with pseudo-time derivative:

$$\frac{\partial \boldsymbol{U}^*}{\partial \tau_f}+\tilde{\omega}\boldsymbol{D}\boldsymbol{U}^*+\frac{\partial \boldsymbol{F}^*}{\partial x}+\frac{\partial \boldsymbol{G}^*}{\partial y}+\frac{\partial \boldsymbol{H}^*}{\partial z}=\boldsymbol{S}^*$$

$$\boldsymbol{D}_{N=2}=\begin{bmatrix} 0.0000 & 0.8507 & -0.5257 & 0.5257 & -0.8507\\ -0.8507 & 0.0000 & 0.8507 & -0.5257 & 0.5257\\ 0.5257 & -0.8507 & 0.0000 & 0.8507 & -0.5257\\ -0.5257 & 0.5257 & -0.8507 & 0.0000 & 0.8507\\ 0.8507 & -0.5257 & 0.5257 & -0.8507 & 0.0000 \end{bmatrix}$$

Hall et al. (2002, 2013) , Ekici and Huang (2012)

THE UNIVERSITY OF TENNESSEE KNOXVILLE

Structural Dynamics Equations

Original structural dynamics equation:

$$\boldsymbol{M}\ddot{\boldsymbol{q}} + \boldsymbol{T}\dot{\boldsymbol{q}} + \boldsymbol{K}\boldsymbol{q} = \boldsymbol{P}(\boldsymbol{q}, t)$$

$$\tilde{\omega}^2 \boldsymbol{D}^2 \boldsymbol{M}^* \boldsymbol{q}^* + \tilde{\omega} \boldsymbol{D} \boldsymbol{T}^* \boldsymbol{q}^* + \boldsymbol{T}^* \boldsymbol{q}^* - \boldsymbol{P}^* = 0$$

Unstable when solved in pseudo-time !

State-space formulation:

$$\dot{\boldsymbol{\eta}} + \boldsymbol{A}\boldsymbol{\eta} + \boldsymbol{R}\boldsymbol{f} = 0$$

$$\boldsymbol{\eta} = \begin{bmatrix} \boldsymbol{q} \\ \dot{\boldsymbol{q}} \end{bmatrix}, \quad \boldsymbol{A} = \left[\begin{array}{c|c} \boldsymbol{0} & -\boldsymbol{I} \\ \hline \boldsymbol{M}^{-1}\boldsymbol{K} & \boldsymbol{M}^{-1}\boldsymbol{T} \end{array}\right], \quad \boldsymbol{R} = \left[\begin{array}{c|c} \boldsymbol{0} & \boldsymbol{0} \\ \hline \boldsymbol{0} & -\boldsymbol{M}^{-1} \end{array}\right], \quad \boldsymbol{f} = \begin{bmatrix} \boldsymbol{0} \\ \boldsymbol{P} \end{bmatrix}$$

Approximate time derivative by pseudo-spectral operator:

$$\tilde{\omega}\boldsymbol{D}\boldsymbol{\eta}^* + \boldsymbol{A}^*\boldsymbol{\eta}^* + \boldsymbol{R}^*\boldsymbol{f}^* = 0$$

Equation with pseudo-time derivative:

$$\frac{\partial \boldsymbol{\eta}^*}{\partial \tau_s} + \tilde{\omega}\boldsymbol{D}\boldsymbol{\eta}^* + \boldsymbol{A}^*\boldsymbol{\eta}^* + \boldsymbol{R}^*\boldsymbol{f}^* = 0$$

The "One-Shot" Approach

Equation with pseudo-time derivative:

$$\frac{\partial \boldsymbol{\eta}^*}{\partial \tau_s} + \tilde{\omega}\boldsymbol{D}\boldsymbol{\eta}^* + \boldsymbol{A}^*\boldsymbol{\eta}^* + \boldsymbol{R}^*\boldsymbol{f}^* = \boldsymbol{0}$$

- The essence of the One-shot approach is to determine the value of the reduced frequency by minimizing the residual of the structural dynamics equation using an optimization.
  - The structural dynamics equation is much simpler (ODE) to deal with
  - It can be solved using a very efficient implicit Euler method with a global "Structural" pseudo timestep allowing values as high as 100.
  - The difficulty due to the nonlinearity (the term *f* due to the generalized aerodynamic forces) in the ODE can be mitigated by lagging the term by one pseudo time iteration.
- **The resulting technique is very efficient with computational times that are orders of magnitude smaller than a time-accurate approach.**

$$Z(\tilde{\omega}) = \frac{1}{2}|\tilde{\omega}\boldsymbol{D}\boldsymbol{\eta} + \boldsymbol{A}\boldsymbol{\eta} + \boldsymbol{R}\boldsymbol{f}|^2 \longrightarrow \tilde{\omega}_{\text{new}} = -\frac{[\boldsymbol{\eta}^T\boldsymbol{A}^T + \boldsymbol{f}^T\boldsymbol{R}^T]\boldsymbol{D}\boldsymbol{\eta}}{\boldsymbol{\eta}^T\boldsymbol{D}^T\boldsymbol{D}\boldsymbol{\eta}}$$

Aeroelastic Governing Equations

Fluid Dynamics

$$\frac{\partial \boldsymbol{U}^*}{\partial \tau_f} + \tilde{\omega}\boldsymbol{D}\boldsymbol{U}^* + \frac{\partial \boldsymbol{F}^*}{\partial x} + \frac{\partial \boldsymbol{G}^*}{\partial y} + \frac{\partial \boldsymbol{H}^*}{\partial z} = \boldsymbol{S}^*$$

$$\frac{\partial \boldsymbol{U}}{\partial \tau_f} + \mathcal{R}_f \left(\underbrace{M_\infty, Re_\infty}_{\text{Fixed parameters}}, \boldsymbol{\eta}(\bar{q}_r,\ \phi_r,\ r \in [1, R]), \tilde{\omega} \right) = \mathbf{0}$$

Structure Dynamics

$$\frac{\partial \boldsymbol{\eta}^*}{\partial \tau_s} + \tilde{\omega}\boldsymbol{D}\boldsymbol{\eta}^* + \boldsymbol{A}^*\boldsymbol{\eta}^* + \boldsymbol{R}^*\boldsymbol{f}^* = \mathbf{0}$$

$$\frac{\partial \boldsymbol{\eta}}{\partial \tau_s} + \mathcal{R}_s \left(\underbrace{\boldsymbol{M}, \boldsymbol{T}, \boldsymbol{K}, \mu}_{\text{Fixed parameters}}, \boldsymbol{f}(\boldsymbol{U}), \tilde{V}, \tilde{\omega} \right) = \mathbf{0}$$

Compact form: $\mathcal{F}\left(\boldsymbol{f},\ \boldsymbol{\eta}(\bar{q}_r,\ \phi_r,\ r \in [1, R]),\ \tilde{V},\ \tilde{\omega} \right) = \mathbf{0}$

Assume both flow and structural vibrations share the same frequency, i.e. frequency "lock-in"

Flowchart of the One-Shot Method

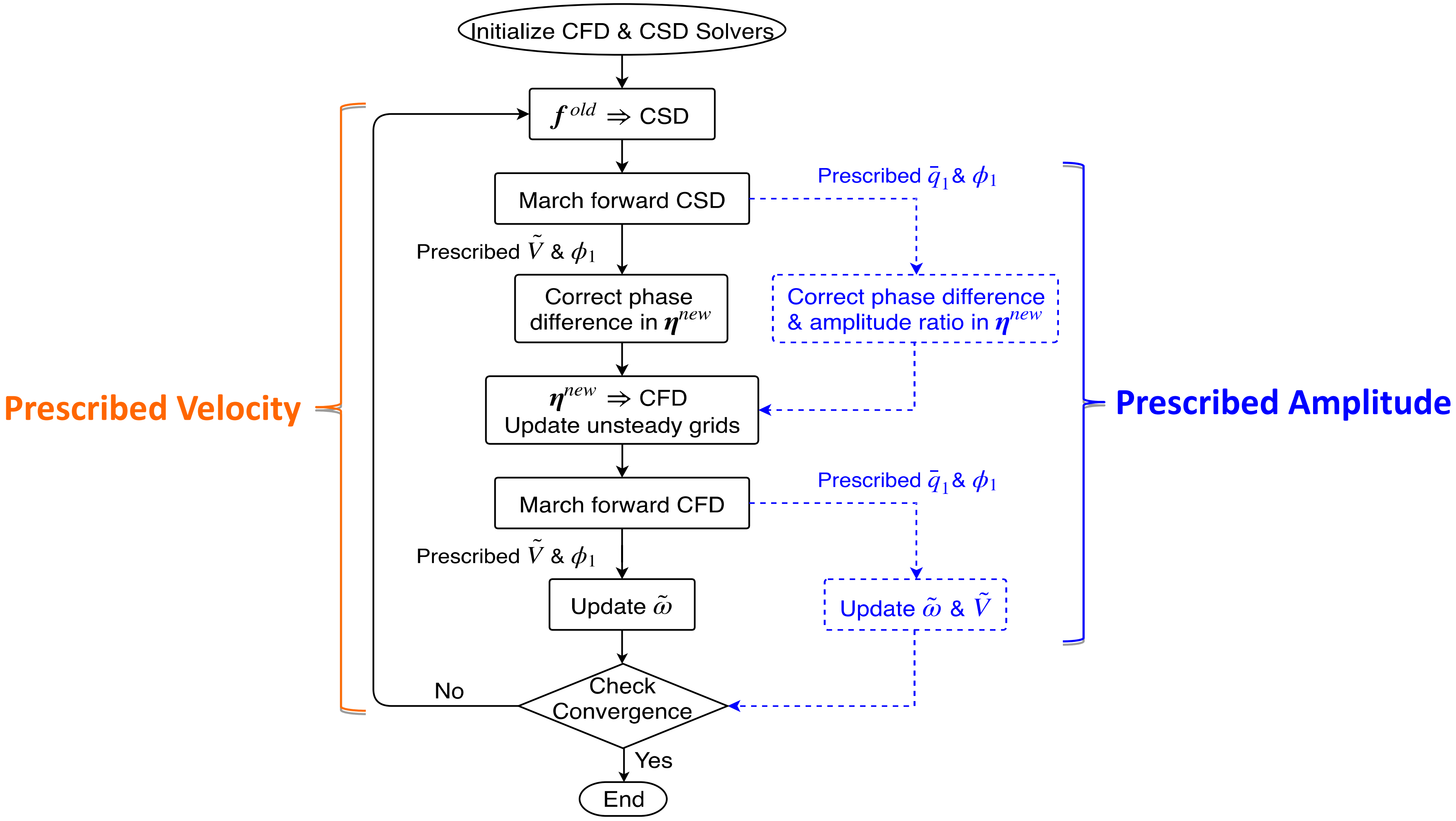

Computational Aeroelasticity Results

1-DOF VIV

2-DOF Pitch-Plunge Airfoils

AGARD 445.6 Wing

COMPUTATIONAL FLUID DYNAMICS
LABORATORY

THE UNIVERSITY OF
TENNESSEE
KNOXVILLE

One-Shot Aeroelastic Results

1-DOF Vortex Induced Vibration (VIV)

- **Elastically Supported Circular Cylinder in Two-Dimensional Laminar Cross-Flow**

Anagnostopoulos and Bearman (1996)

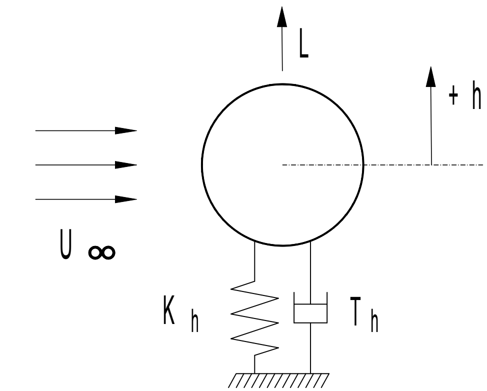

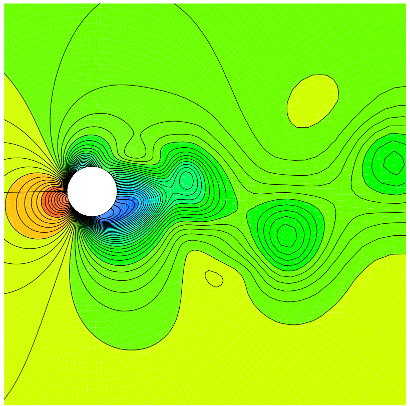

- **Vortex shedding remains 2D and laminar**

  $Re_\infty \leq 180$

- **Strouhal frequency is used**

  $St = \tilde{\omega}/2\pi$

- **Constant damping and linear elasticity**

$$m_h \ddot{h} + T_h \dot{h} + K_h h = q_\infty D s C_l$$

$$\tilde{h}'' + \zeta_h \frac{4\pi}{\kappa Re} \tilde{h}' + \frac{4\pi^2}{\kappa^2 Re_\infty^2} \tilde{h} = \frac{2}{\pi\mu} C_l \qquad (\zeta_h = 0.00136; \quad \kappa = 0.049772; \quad \mu = 149.0913)$$

Nondimensionalized in terms of *Reynolds number* which functions similarly to the reduced velocity

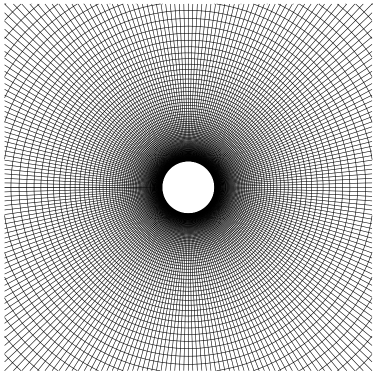

257×129

(Carlson et al., 2005; Besem et al., 2016)

One-Shot Aeroelastic Results

1-DOF Vortex Induced Vibration (VIV)

- **Case 1:** $Re_\infty = 110$
- **Sweep over the *Reynolds number* and determine the LCO conditions (amplitude/frequency) of the system using the one-shot approach**

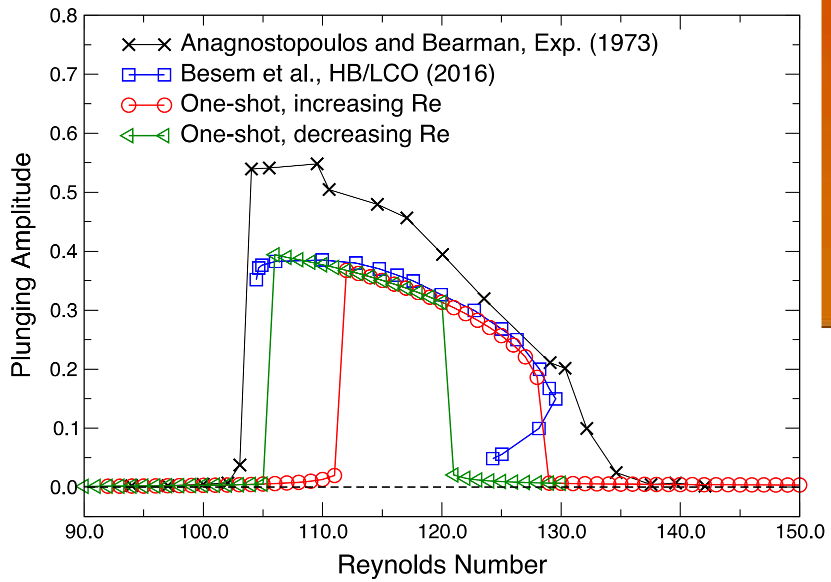

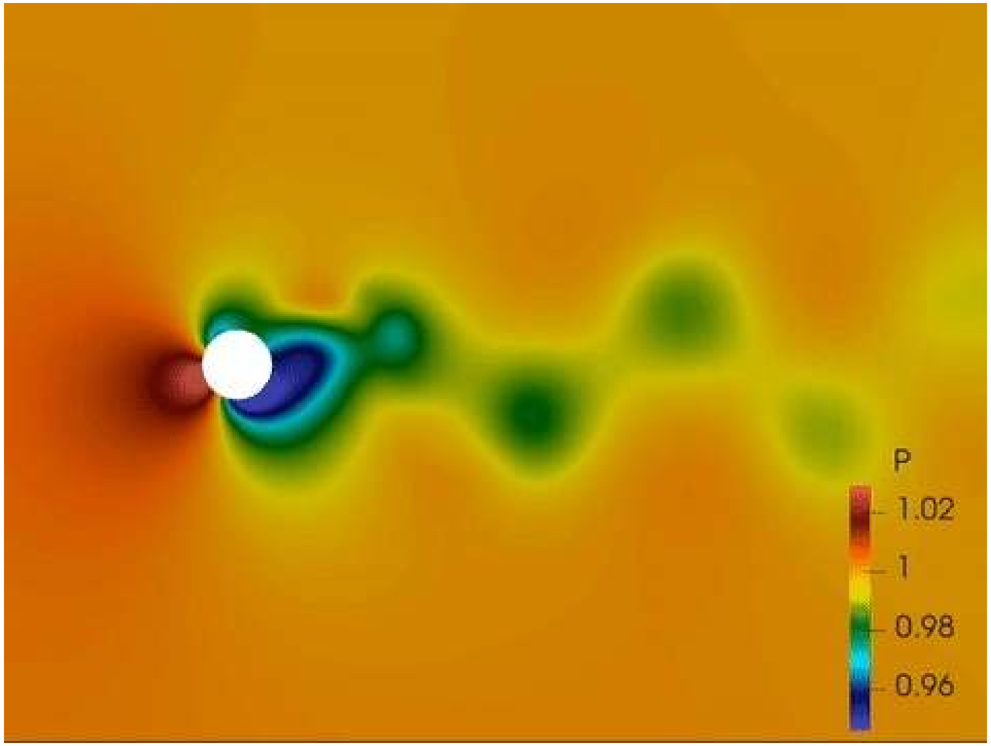

Aeroelastic Results

2-DOF Pitch-Plunge Airfoil

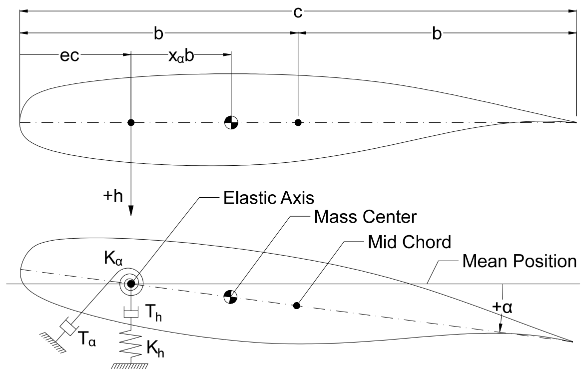

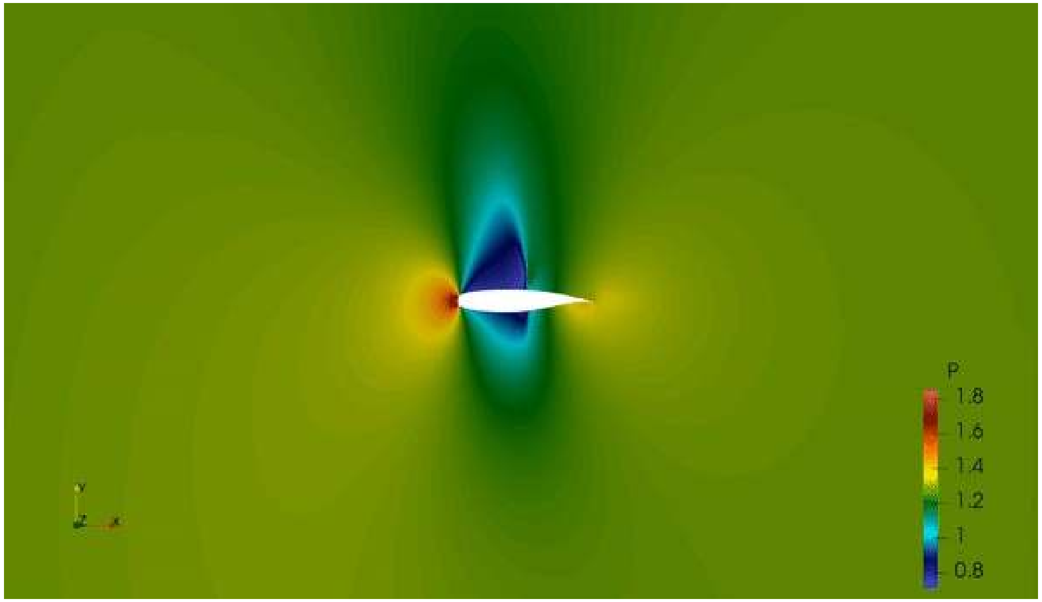

Static equation: $$K_\alpha(\alpha_0 - \alpha_{e0}) = q_\infty c^2 s C_{m0}$$

Unsteady equations:
$$m_h\ddot{h} + S_\alpha\ddot{\alpha} + T_h\dot{h} + K_h h = -q_\infty c s C_l$$
$$S_\alpha\ddot{h} + I_\alpha\ddot{\alpha} + T_\alpha\dot{\alpha} + K_\alpha\alpha = q_\infty c^2 s C_m$$

	LCO, Schewe and Deyhle (1996)	Flutter, Isogai (1979,1981)
airfoil geometry	supercritical NLR 7301	symmetric NACA 64A010
plunging mass-wing mass ratio, m_h/m_0	5.729	1.0
elastic axis position, e	0.25	-0.5
airfoil static unbalance, x_α	0.555	1.8
radius of gyration (squared), r_α^2	0.822	3.48
natural frequency ratio, ω_h/ω_α	1.83	1.0
plunge damping coefficient, ζ_h	0.0175	0.0
pitch damping coefficient, ζ_α	0.00411	0.0
mass ratio, μ	172.0	60.0
freestream Mach number, Ma_∞	0.75	multiple Mach numbers
flow condition	viscous & turbulent	inviscid

Aeroelastic Results

2-DOF NLR 7301 Airfoil

Prescribing velocity:

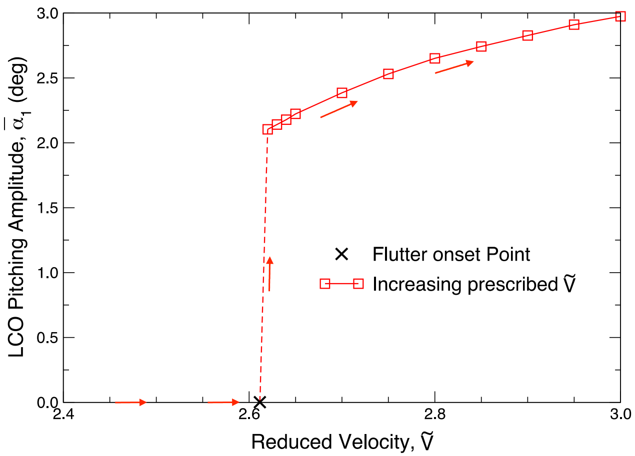

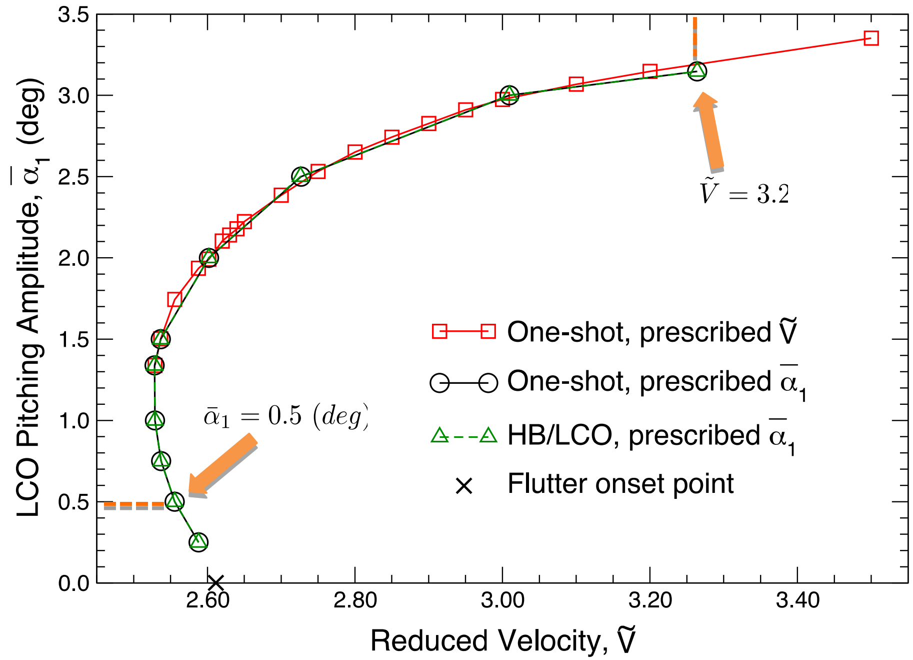

Prescribing amplitude:

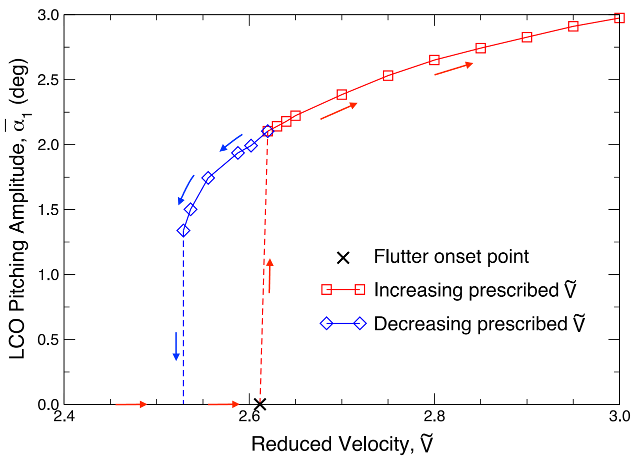

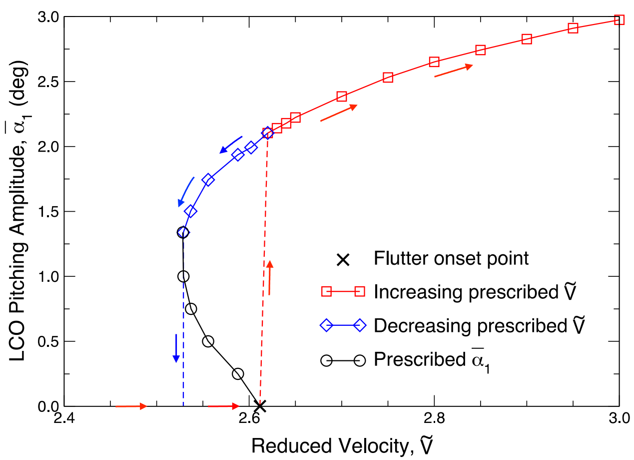

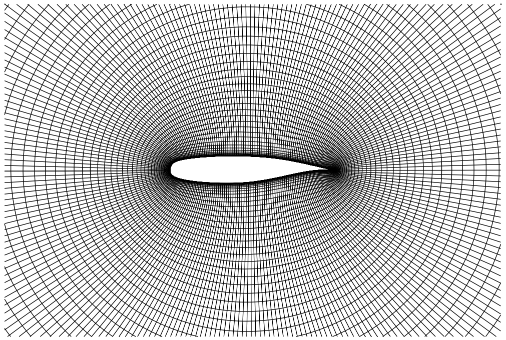

257×129 viscous mesh

Computational Efficiency

2-DOF NLR 7301 Airfoil

➢ **Stable LCO condition** $\tilde{V} = 3.2$

Compared to the HB/LCO method:

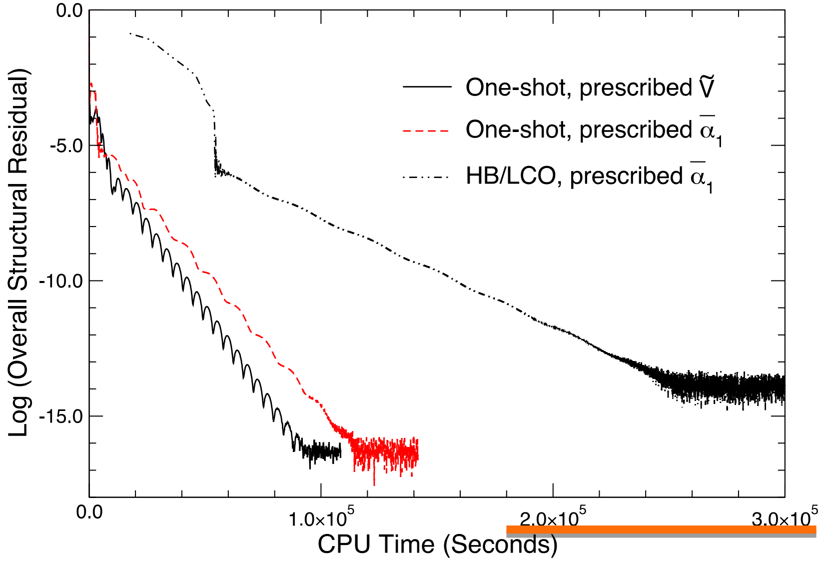

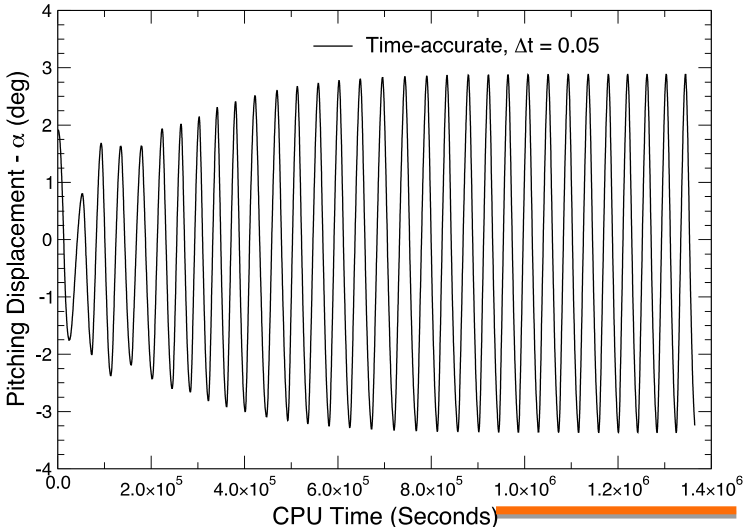

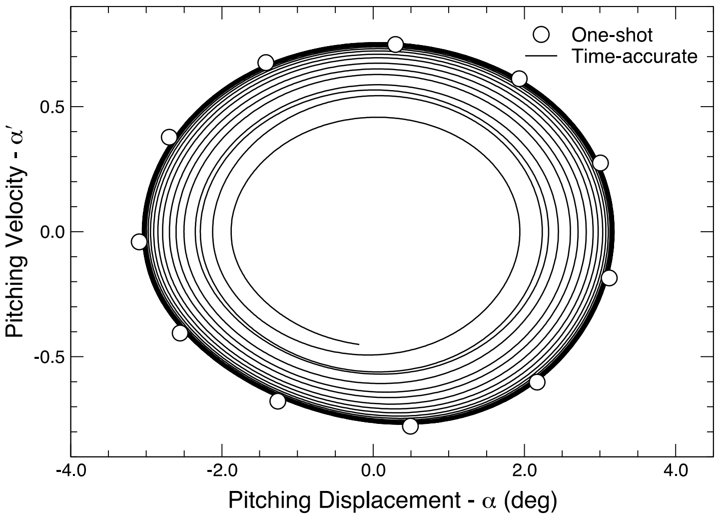

Time-accurate results

CFD THE UNIVERSITY OF TENNESSEE KNOXVILLE

Aeroelastic Results

2-DOF NACA 64A010 Airfoil

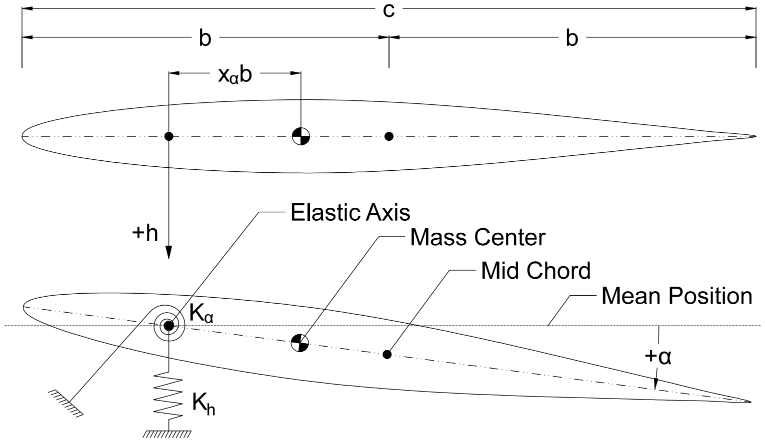

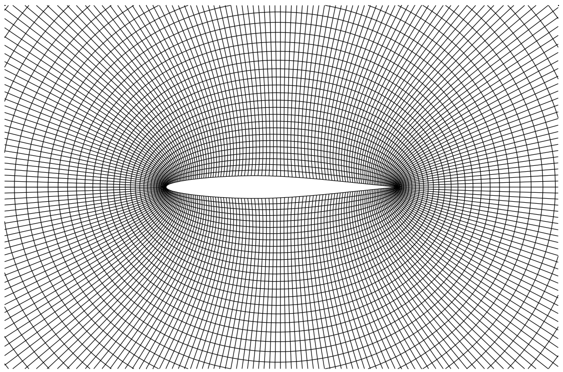

257×129 inviscid mesh

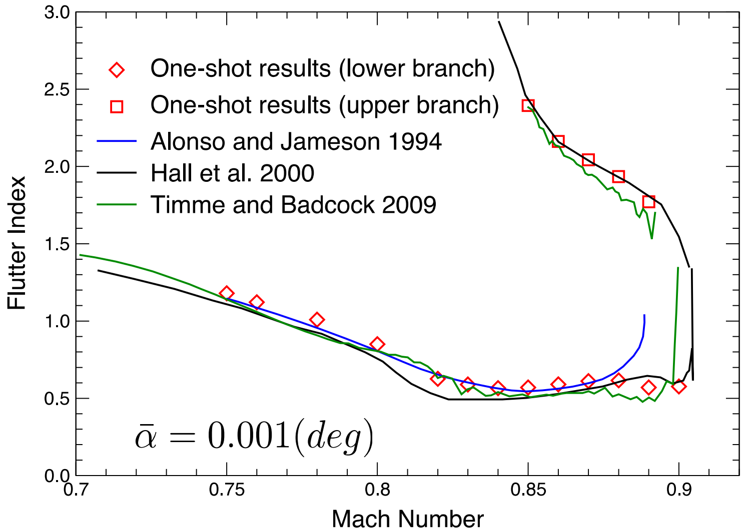

Aeroelastic Results

Flutter Prediction for AGARD 445.6 Wing

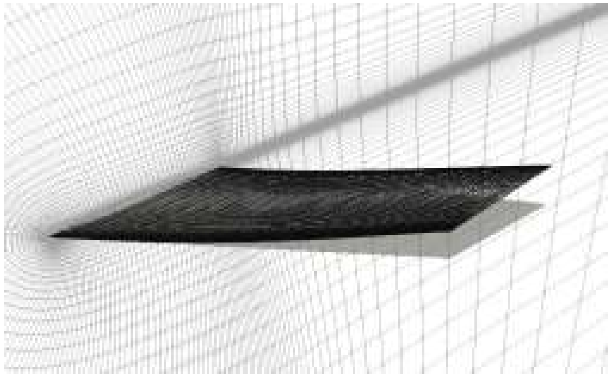

Mode 1 (first bending) - 9.6 Hz

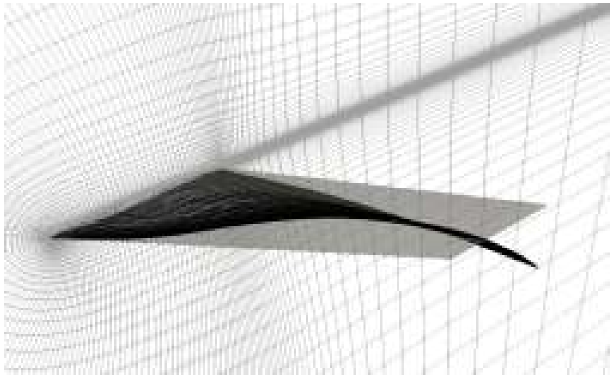

Mode 2 (first torsion) - 38.1 Hz

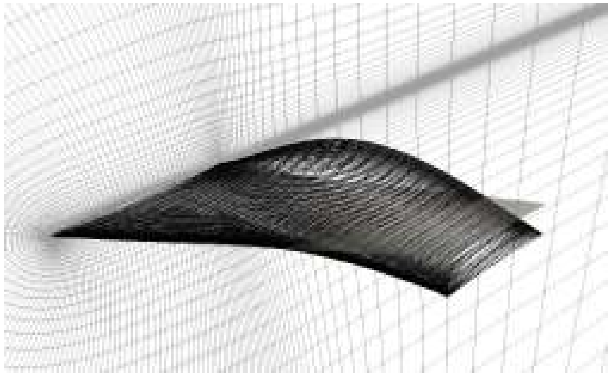

Mode 3 (second bending) - 50.7 Hz

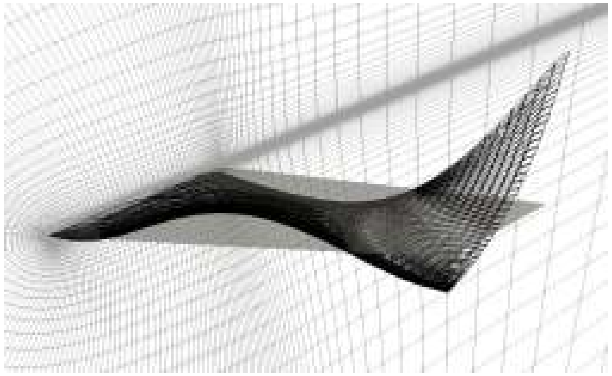

Mode 4 (second torsion) - 98.5 Hz

Yates (1963, 1985)

Aeroelastic Results

Flutter Prediction for AGARD 445.6 Wing

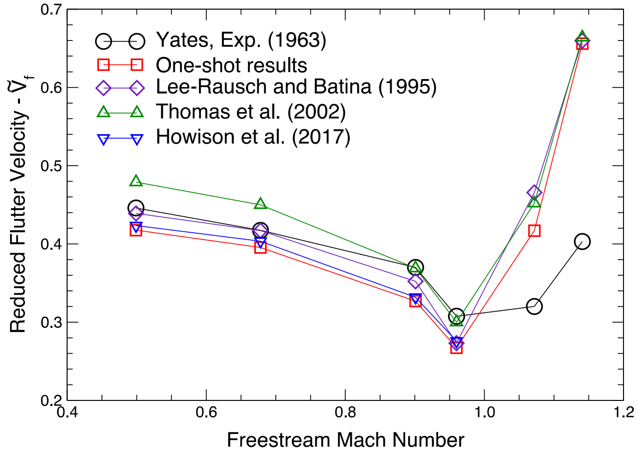

Validation of One-shot Method Results

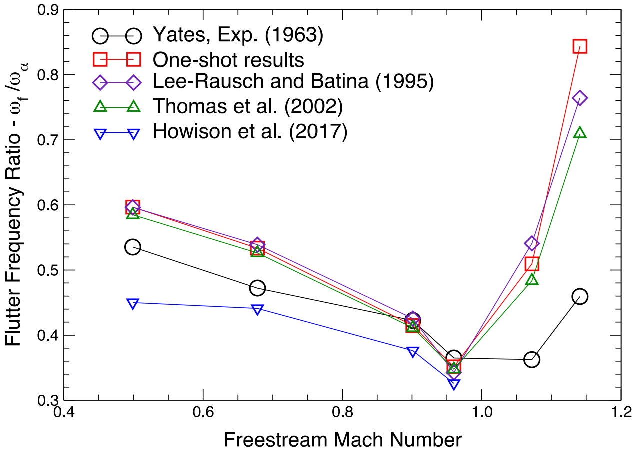

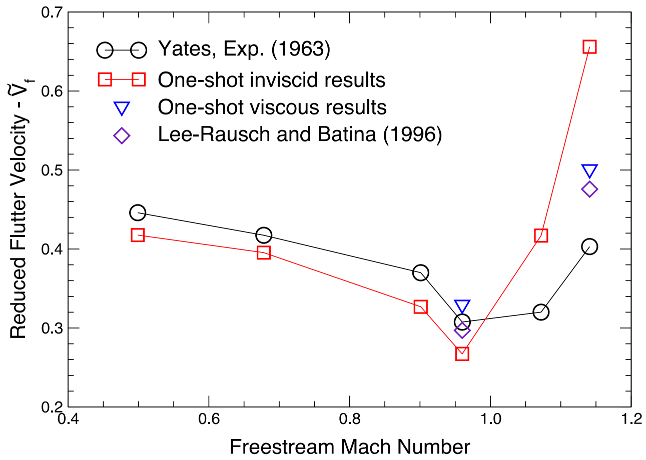

Comparison of Inviscid and Viscous Results

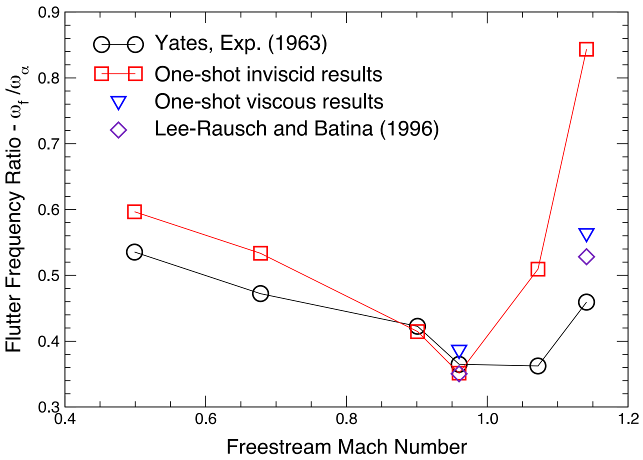

Aeroelastic Results

Flutter Prediction for AGARD 445.6 Wing

Comparison of Inviscid and Viscous Surface Pressure Distributions

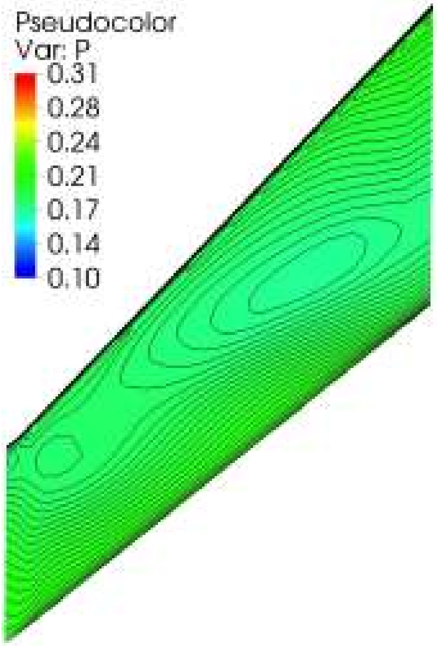

$M_\infty = 0.960$, Inviscid

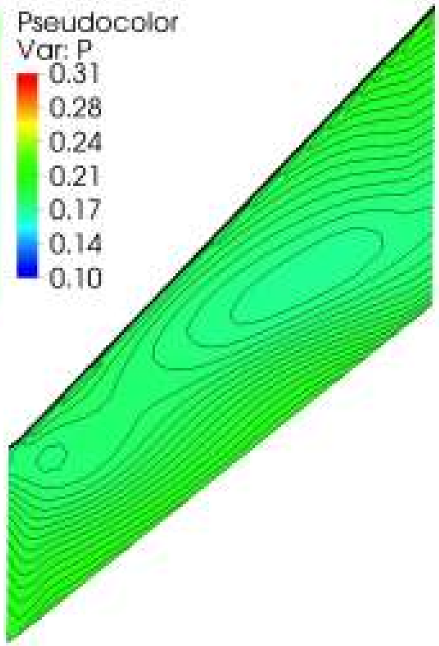

$M_\infty = 0.960$, Viscous

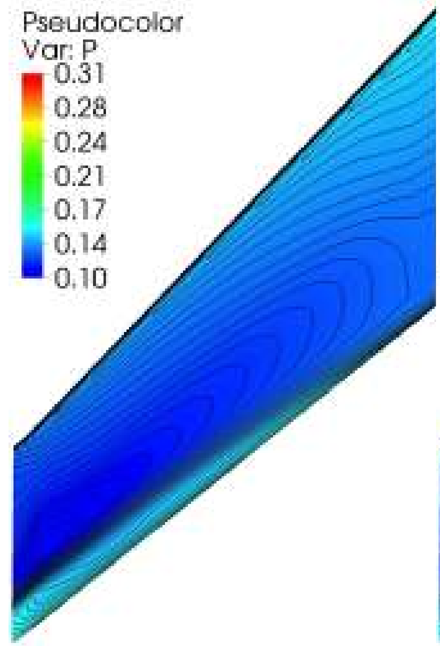

$M_\infty = 1.141$, Inviscid

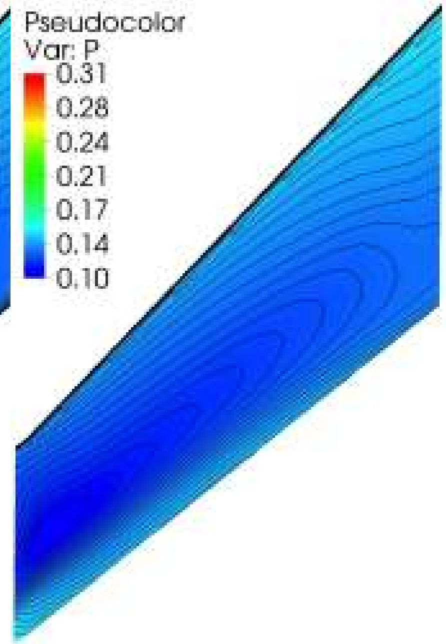

$M_\infty = 1.141$, Viscous

Aeroelastic Results

Flutter Prediction for AGARD 445.6 Wing

LCO response $M_\infty = 0.960,\ \bar{q}_1 = 0.01$

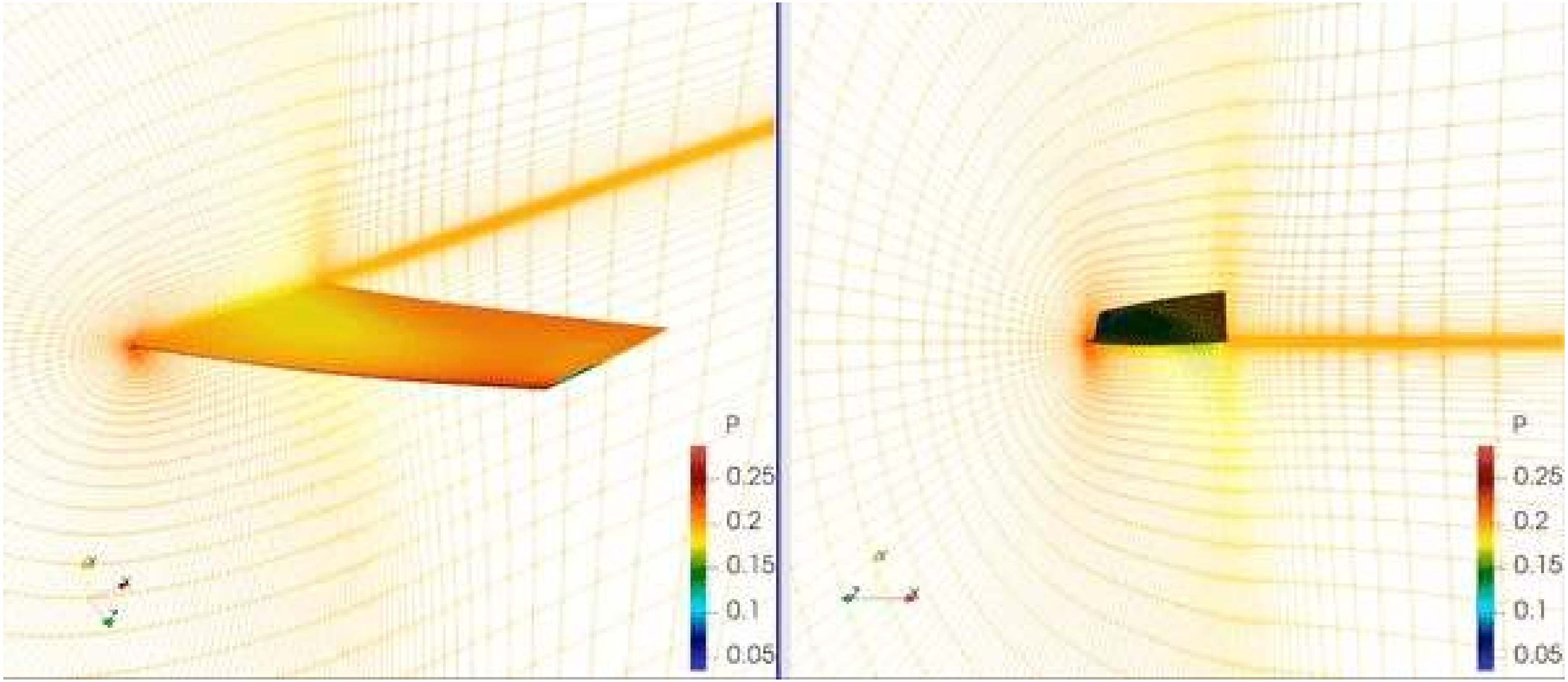

Aerodynamic Design Optimization

Introduction

COMPUTATIONAL FLUID DYNAMICS
LABORATORY

THE UNIVERSITY OF TENNESSEE
KNOXVILLE

Aerodynamic Design Optimization

➢ Computational Fluid Dynamics (CFD):

- Low-Fidelity: Blade-Element-Momentum
- Moderate-Fidelity: Euler and Navier-Stokes Solvers
- High-Fidelity: **(U)RANS** Solvers, DES, LES, DNS

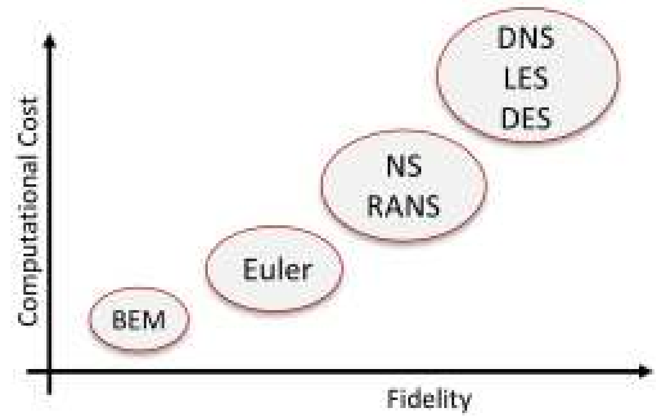

➢ Design Optimization:

- **Non-Gradient-Based**
  - Evolution Strategies, Genetic Algorithms, Random Search
    - Repeated cost function evaluations

"**evolved antenna**" for 2006 NASA ST5 spacecraft designed using an evolutionary algorithm

- **Gradient-Based**
  - Iterative solution of nonlinear programming problems
    - Faster convergence (less design cycles)
    - **Sensitivity (gradient) information is required**

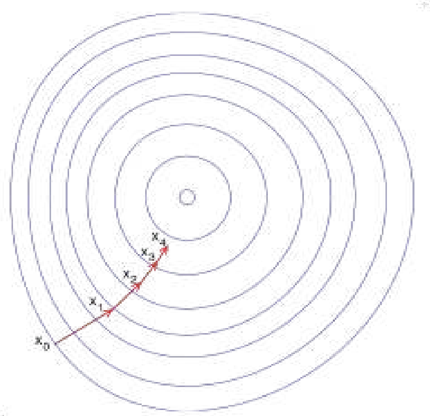

"**gradient descent**" approach

Aerodynamic Design Optimization

- Grid-Transparent Unstructured Parallel Solver
- Reynolds-Averaged Navier-Stokes (RANS) Eqn's + S-A Turbulence and B-C Transition Models
- Steady, Time-Accurate, Time-Periodic (HB)

- Fast and Fully-Automated Discrete Adjoint Sensitivity Analysis
- Operator-Overloading Technique with OOP
- Computationally and Memory Efficient
- Easy Implementation into any Solver

UNPAC
Design Optimization
Framework

UNPAC-DOF

1) UNPAC Solver

Governing Equations

- Reynolds-Averaged Navier-Stokes Equations: $$\frac{\partial}{\partial t}\int_{\mathcal{V}} \vec{U}\, d\mathcal{V} + \oint_{\partial\mathcal{V}} \left[\vec{F}_c - \vec{F}_v\right]\, dS = \int_{\mathcal{V}} \vec{Q}\, d\mathcal{V}$$

where

Conservation Variables
$$\vec{U} = [\rho, \rho\vec{v}, \rho E, \rho\tilde{\nu}]^{\mathrm{T}}$$

$$\vec{F}_c = \begin{bmatrix} \rho V \\ \rho u V + p\, n_x \\ \rho v V + p\, n_y \\ \rho w V + p\, n_z \\ \rho H V \\ \rho\tilde{\nu} V \end{bmatrix} \quad \vec{F}_v = \begin{bmatrix} 0 \\ \vec{\tau}_{x_1}\cdot\vec{n} \\ \vec{\tau}_{x_2}\cdot\vec{n} \\ \vec{\tau}_{x_3}\cdot\vec{n} \\ \vec{\Theta}\cdot\vec{n} \\ \vec{\tau}^{SA}_{x_i x_i}\cdot\vec{n} \end{bmatrix} \quad \vec{Q} = \begin{bmatrix} 0 \\ \rho f_{e,x} \\ \rho f_{e,y} \\ \rho f_{e,z} \\ \rho\vec{f}_e\cdot\vec{v} \\ Q^{SA} \end{bmatrix}$$

Convective Flux — Viscous Flux — Source Terms

Continuity
x-Momentum
y-Momentum
z-Momentum
Energy
Spalart-Allmaras

Flux-Difference Splitting (Roe scheme)
1st order & 2nd order
(w/ Venkatakrishnan's limiter function)

Central Averaging (2nd order)
(Corrected face averaging of gradients)

Volumetric (nodal)
External forces defined by "Coriolis" and "Centrifugal" terms for RFR

$$\boxed{\frac{\partial \mathcal{V}_i \vec{U}_i}{\partial t} + \vec{R}_i = 0}$$

semi-discretized RANS equations

2) FDOT Toolbox

Operator-Overloading and OOP

- Overloading operators:
  - Considering
    $$y = x_1 \cos(x_2)$$
  - Recording "expression tree"

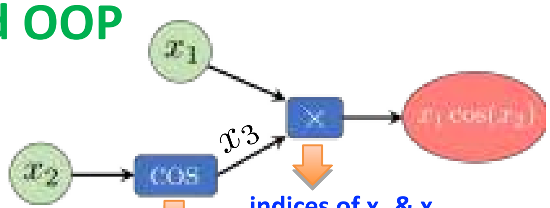

index of x_2
OPT_COS

indices of x_1 & x_3
OPT_MUL

$$
\begin{aligned}
x_1 &= x_1 \\
x_2 &= x_2 \\
x_3 &= \cos(x_2) \\
y &= x_1 \times x_3
\end{aligned}
$$

AD

$$\bar{y} = 1.0$$

$$
\boxed{\begin{aligned}
\bar{x}_1 &= \bar{x}_1 + x_3\ \bar{y} \\
\bar{x}_3 &= \bar{x}_3 + x_1\ \bar{y}
\end{aligned}}
$$
OPT_MUL

$$\boxed{\bar{x}_2 = \bar{x}_2 - \sin(x_2)\ \bar{x}_3}$$
OPT_COS

2) FDOT Toolbox

Operator-Overloading and OOP

- Overloading operators:
  - Considering
    $y = x_1 \cos(x_2)$
  - Recording "expression tree"

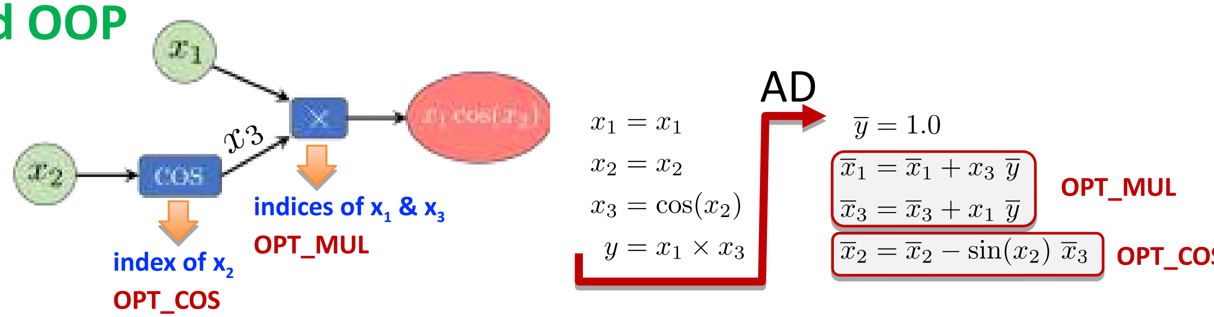

- Primal and Adjoint Operations

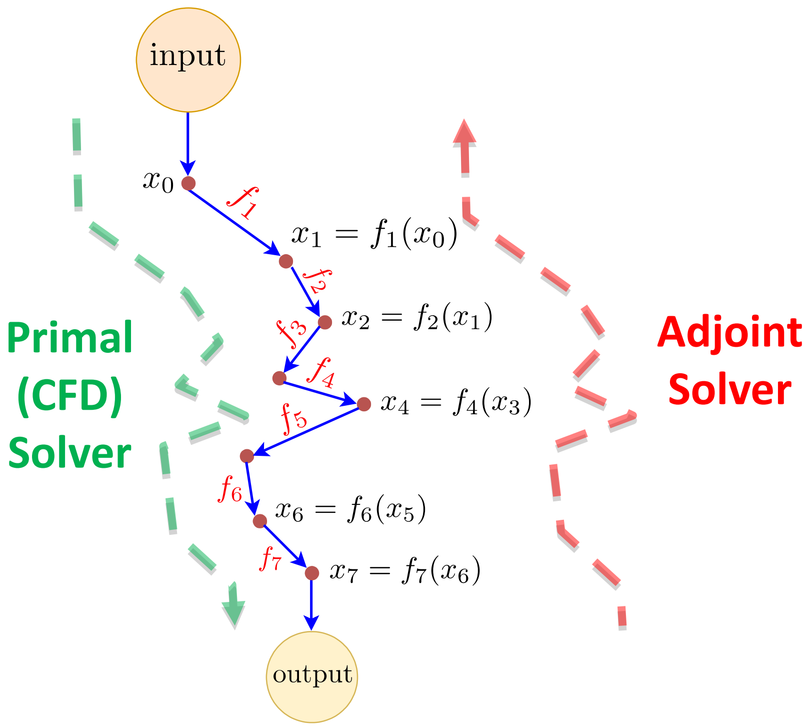

✓ **In the forward (primal) pass, the expression tree, that includes all operations, is recorded to the "tape"**

✓ **In the reverse (adjoint) pass, the recorded tape is rewound and sensitivities/gradients are evaluated.**

2) FDOT Toolbox

Operator-Overloading and OOP

- Overloading operators:
  - Considering
    $$y = x_1 \cos(x_2)$$
  - Recording "expression tree"

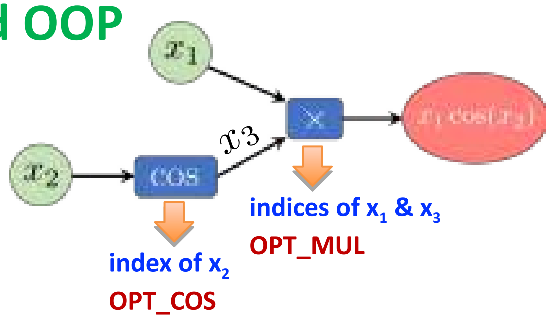

$$x_1 = x_1$$
$$x_2 = x_2$$
$$x_3 = \cos(x_2)$$
$$y = x_1 \times x_3$$

AD

$$\bar{y} = 1.0$$
$$\boxed{\begin{aligned}\bar{x}_1 &= \bar{x}_1 + x_3\,\bar{y}\\ \bar{x}_3 &= \bar{x}_3 + x_1\,\bar{y}\end{aligned}}\quad \text{OPT\_MUL}$$
$$\boxed{\bar{x}_2 = \bar{x}_2 - \sin(x_2)\,\bar{x}_3}\quad \text{OPT\_COS}$$

- Minimal changes need to be made in order to convert the primal code to the adjoint code:

Pseudo-code: Nozzle Flow Solver (<u>primal code</u>)

```
call start_up
call mesh
call flow_initialization

do iter = 1,max_iter
   call one_iteration
end do

call cost_function
```

Pseudo-code: Nozzle Flow Solver (<u>adjoint code</u>)

```
call start_up
call mesh
call load_fully_converged_solution
call FDOT_set_iterative_soln_input(Q)
call FDOT_set_checkpoint

do iter = 1,1
   call one_iteration
   call FDOT_set_iterative_soln_output(Q)
end do

call FDOT_set_checkpoint
call cost_function
call FDOT_set_objective(I)
call FDOT_evaluate_adjoints
```

2) FDOT Toolbox

Implementation

- FDOT Toolbox Module:
  - Module is included in source codes
  - Real variables are replaced by **AReal** type
  - Nominal solver is run and the "**fully-converged**" solution is used to initiate the adjoint solver
  - Using a "***checkpointing***" function, the iterative part of the tape is marked
  - Iterative variables are flagged
  - Adjoint of the cost function is set to unity with all others initialized by zero
  - "**Tape evaluation**" function is called

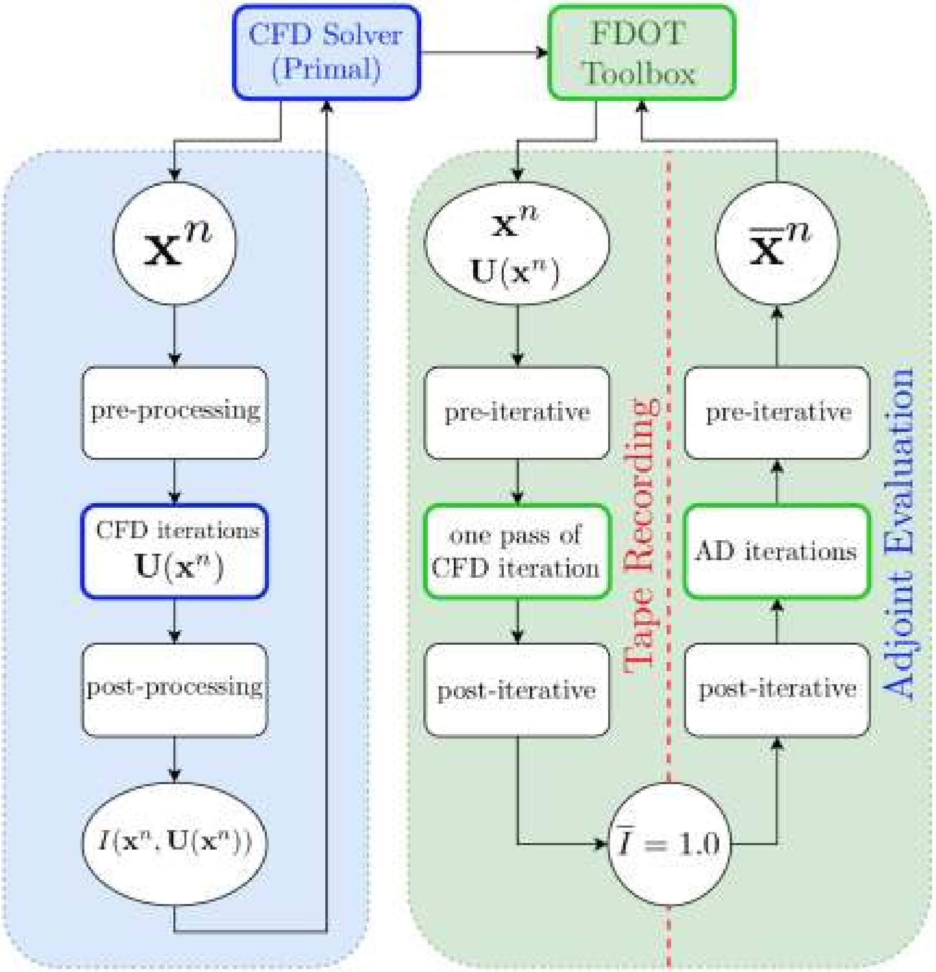

- Djeddi, R., and Ekici, K.. **"FDOT: A Fast, memory-efficient and automated approach for Discrete adjoint sensitivity analysis using the Operator overloading Technique."** *Aerospace Science and Technology 91 (2019): 159-174.*

3) UNPAC-DOF

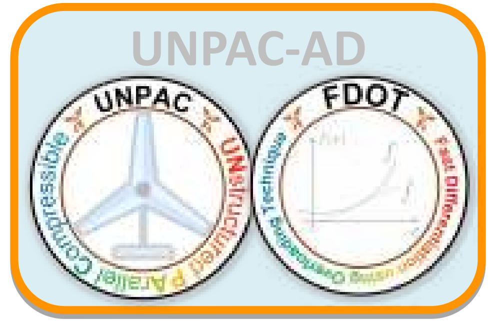

UNPAC-AD

- UNPAC Adjoint Solver:
  - UNPAC solver coupled with the FDOT toolbox

UNPAC-OPT

- Optimizer Program:
  - Unbounded and Bound Constrained Optimization
  - L-BFGS-B Optimizer:

$$\min f(\vec{x})$$

$$\text{subject to} \quad \vec{l} \leq \vec{x} \leq \vec{u}$$

- <u>Objectives:</u>
  - ❑ **Drag (Minimize)**
  - ❑ **Lift (Maximize)**
  - ❑ **Lift/Drag (Maximize)**

Broyden-Fletcher-Goldfarb-Shanno

Shape Deformation/Parameterization

- Surface Grid Points:
  - <u>**Smoothing**</u> process applied to surface perturbations
- Free-Form Deformation (FFD) Box:

$$\Delta x_i = x_i^{n+1} - x_i^n$$

$$\boxed{\Delta x_i^* + \sum_{j=1}^{\mathrm{Ngb}_i} \epsilon \left[\Delta x_i^* - \Delta x_j\right] = \Delta x_i}$$

$$\vec{x}^{n+1} = \vec{x}^n + \Delta\vec{x}^*$$

$$\boxed{\mathbf{x}_s = \sum_{i=0}^{\mathrm{NI}} \sum_{j=0}^{\mathrm{NJ}} \sum_{k=0}^{\mathrm{NK}} B_i^{\mathrm{NI}}(\xi_s)\, B_j^{\mathrm{NJ}}(\eta_s)\, B_k^{\mathrm{NK}}(\zeta_s)\; \mathbf{x}_{\mathrm{cp}}}$$

$$B_p^n(s) = C_p^n s^p (1-s)^{n-p}$$

3) UNPAC-DOF

UNPAC-DOF

➢ Wrapper Program:

- Couples the UNPAC, UNPAC-AD, and UNPAC-OPT programs
- Written in Modern Fortran
- Uses "bash scripting" to organize solution files and folders at each design cycle
- Applies a pseudo-Laplacian to smooth surface perturbations

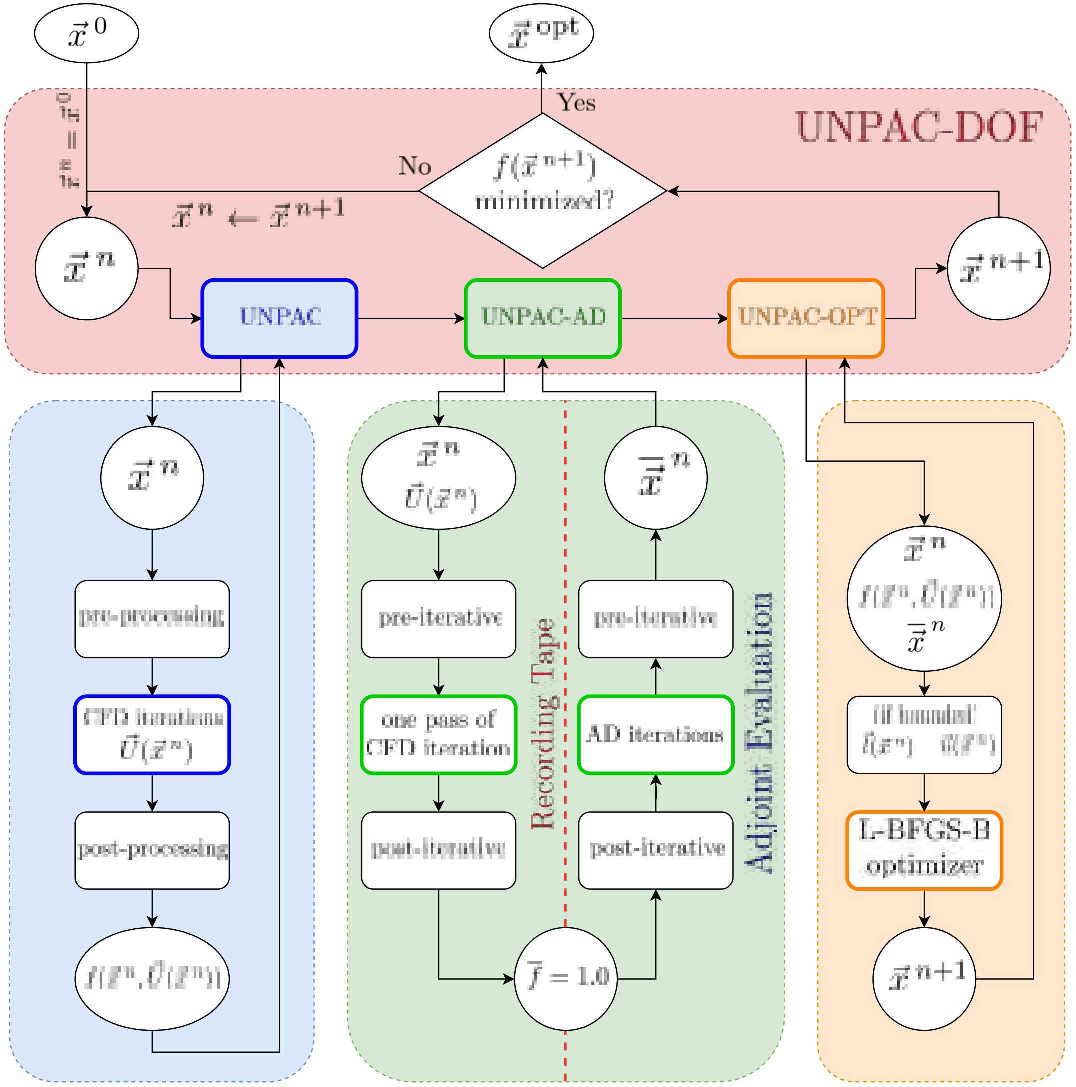

Aerodynamic Design Optimization Results

NACA0012 Airfoil

ONERA M6 Wing

COMPUTATIONAL FLUID DYNAMICS
LABORATORY

THE UNIVERSITY OF
TENNESSEE
KNOXVILLE

Design Optimization Results

NACA0012 Airfoil Subject to Inviscid Transonic Flow

- Drag Minimization:
  - M = 0.8, AoA = 1.25 deg
  - “Surface Points” used as DV’s for deformation

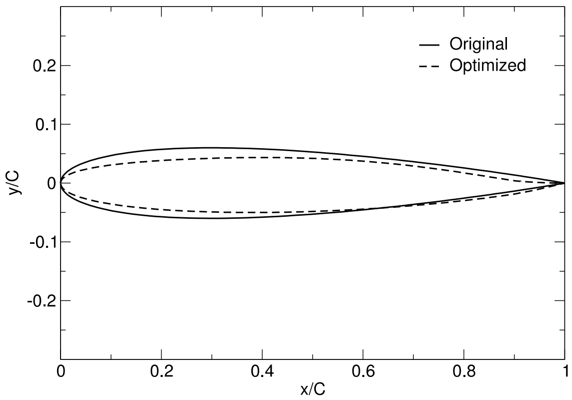

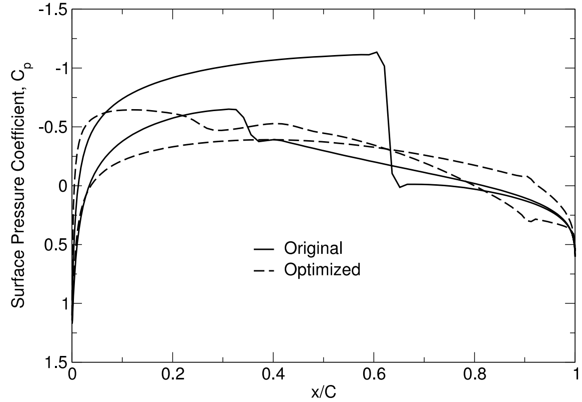

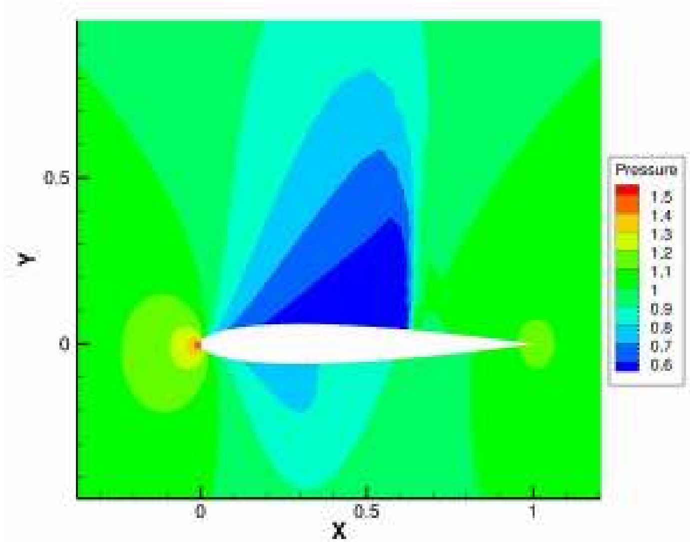

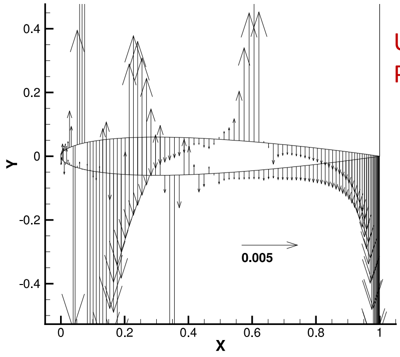

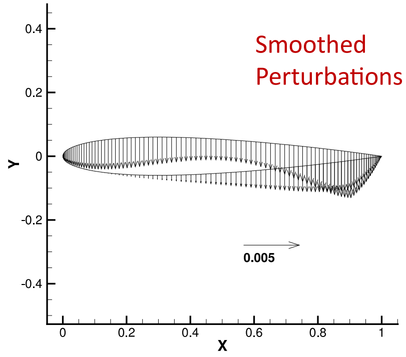

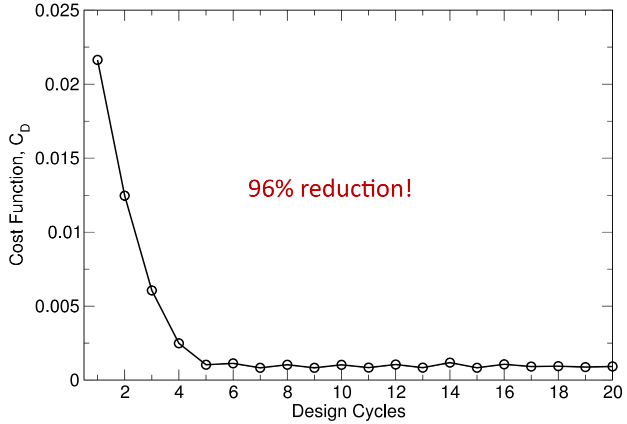

THE UNIVERSITY OF TENNESSEE KNOXVILLE

Design Optimization Results

NACA0012 Airfoil Subject to Inviscid Transonic Flow

- Drag Minimization:
  - M = 0.8, AoA = 1.25 deg
  - “2D FFD Box” used for shape parameterization

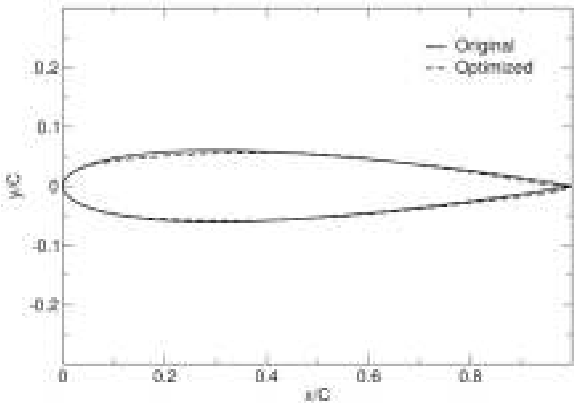

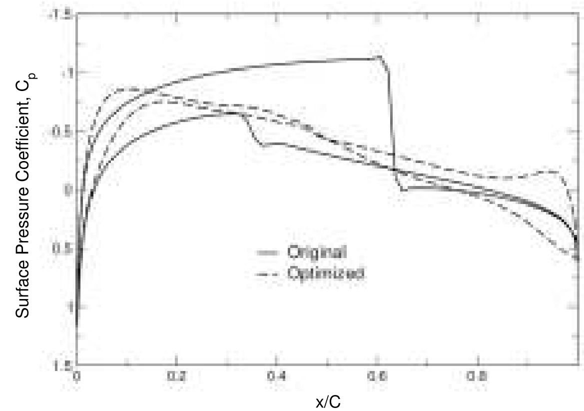

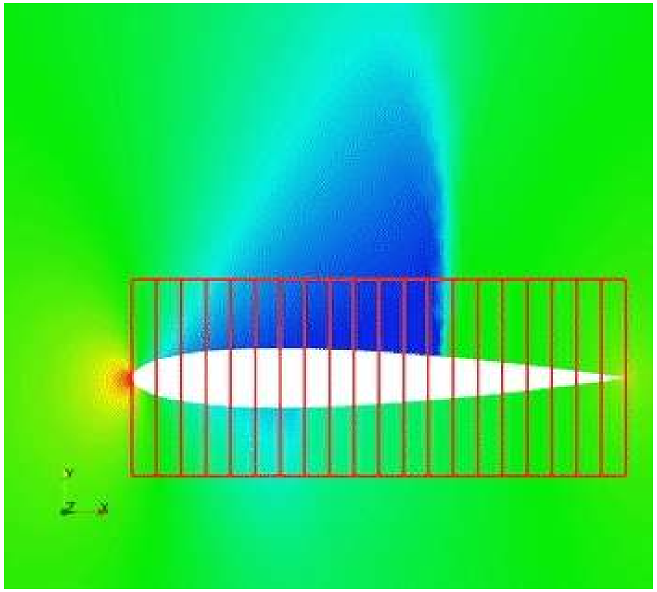

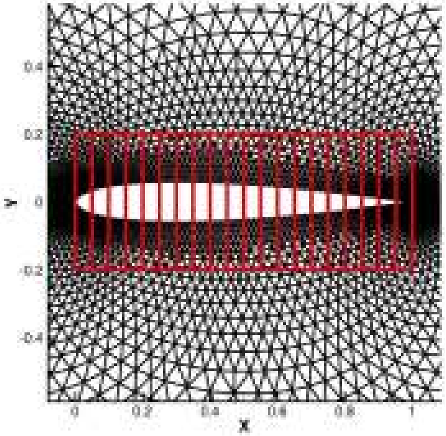

Original
FFD Box

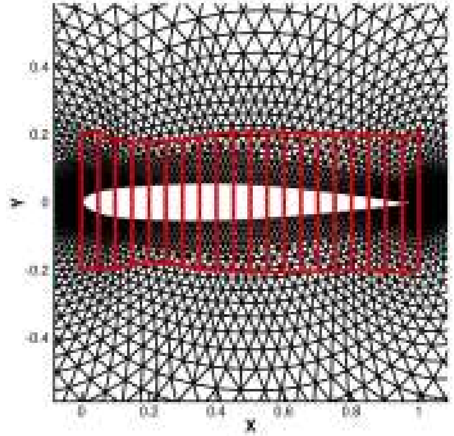

Optimized
FFD Box

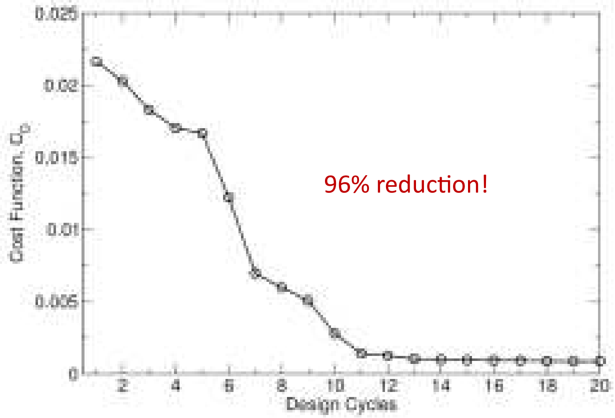

THE UNIVERSITY OF TENNESSEE KNOXVILLE

Design Optimization Results

NACA0012 Airfoil Subject to Inviscid Transonic Flow

- Drag Minimization:
  - M = 0.8, AoA = 1.25 deg
  - Comparison of Shape Parameterization Results

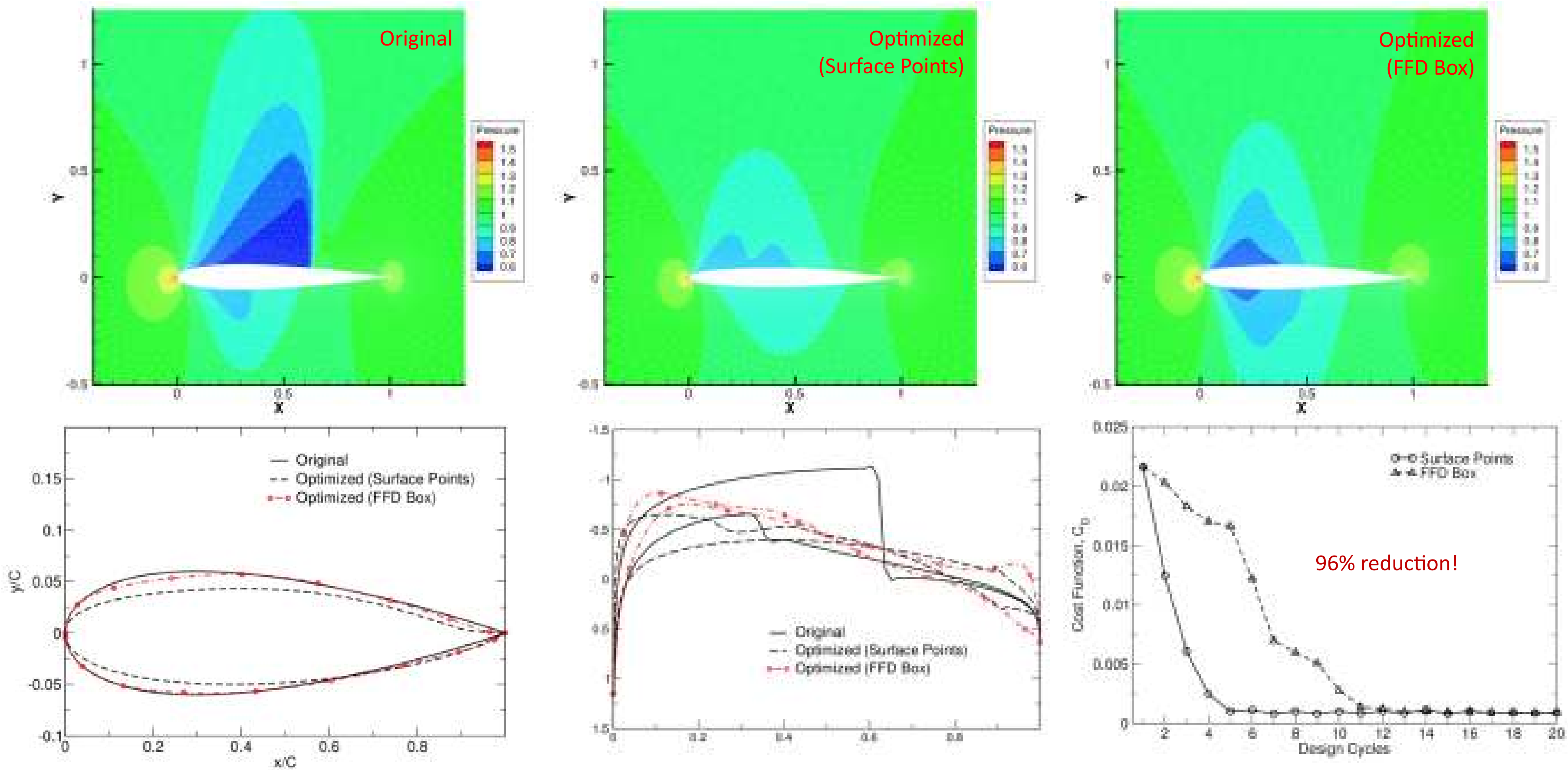

Design Optimization Results

NACA0012 Airfoil Subject to Inviscid Transonic Flow

- Drag Minimization:
  - M = 0.8, AoA = 1.25 deg
  - Comparison of Shape Parameterization Results

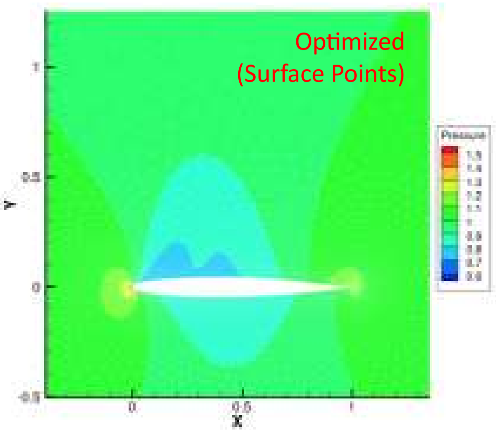

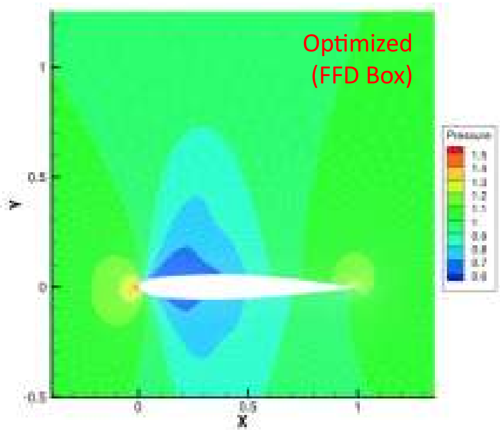

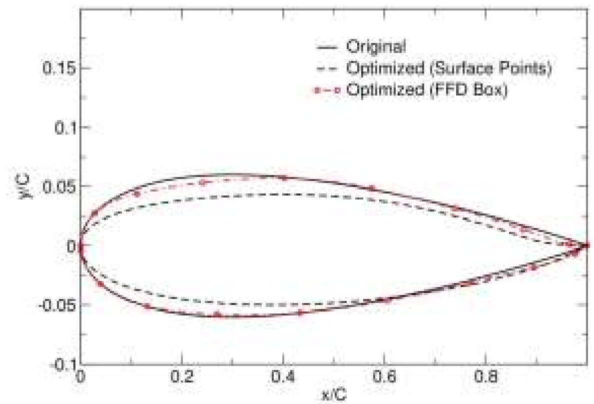

Geometry	C_D	Reduction	t_{max}/c	Reduction
Original	2.1638E-2	-	0.120	-
Optimized (Surface Points)	9.1755E-4	95.7%	0.093	22.5%
Optimized (FFD Box)	8.7265E-4	95.9%	0.115	4.2%

Memory Footprint:
Adjoint Solver -> 800 **Mbytes**

Normalized CPU Time:

Design Optimization Results

ONERA M6 Wing

- Drag Minimization:
  - Based on ONERA D airfoil section (10% t/c)
  - 30 degree sweep angle
  - Aspect Ratio = 3.8, Taper Ratio = 0.562
  - M = 0.8395, AoA = 3.06 deg

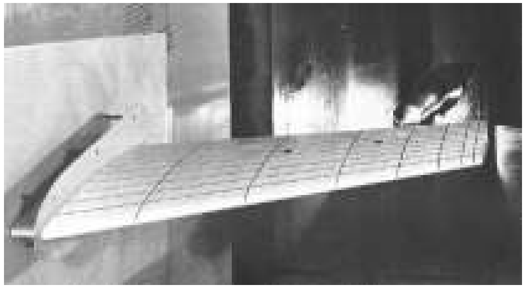

NASA TMR: Schmitt and Charpin (1979)

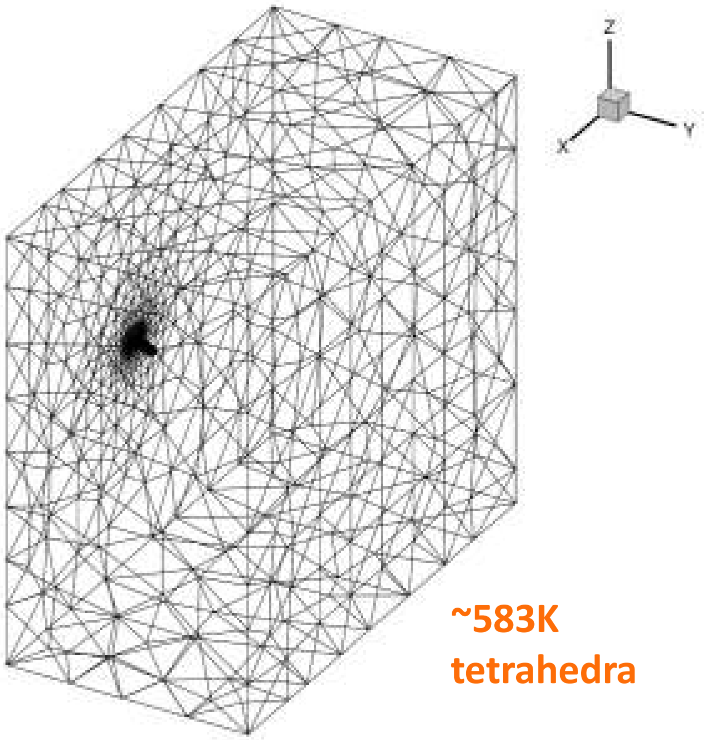

~583K tetrahedra

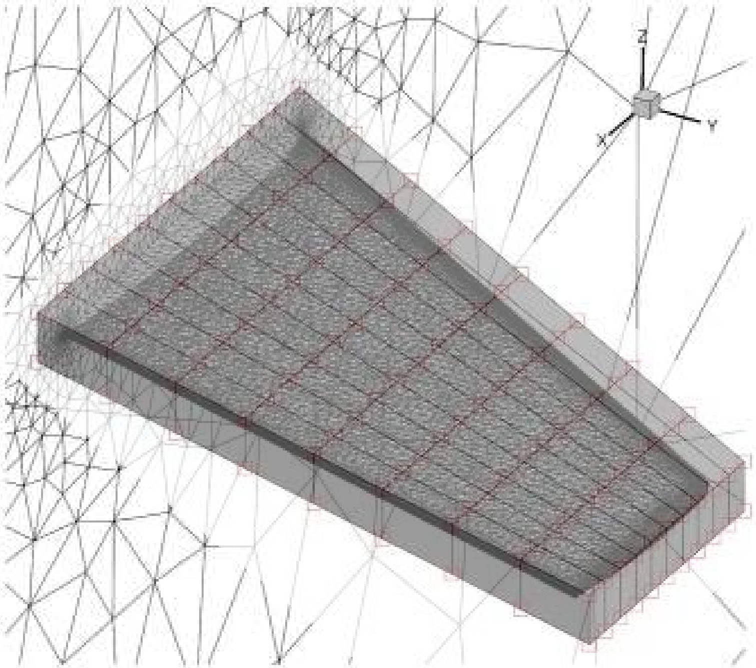

~39K triangles

FFD Box 11x9x2 Control Points

Design Optimization Results

ONERA M6 Wing

- **Drag Minimization:**
  - M = 0.8395, AoA = 3.06 deg

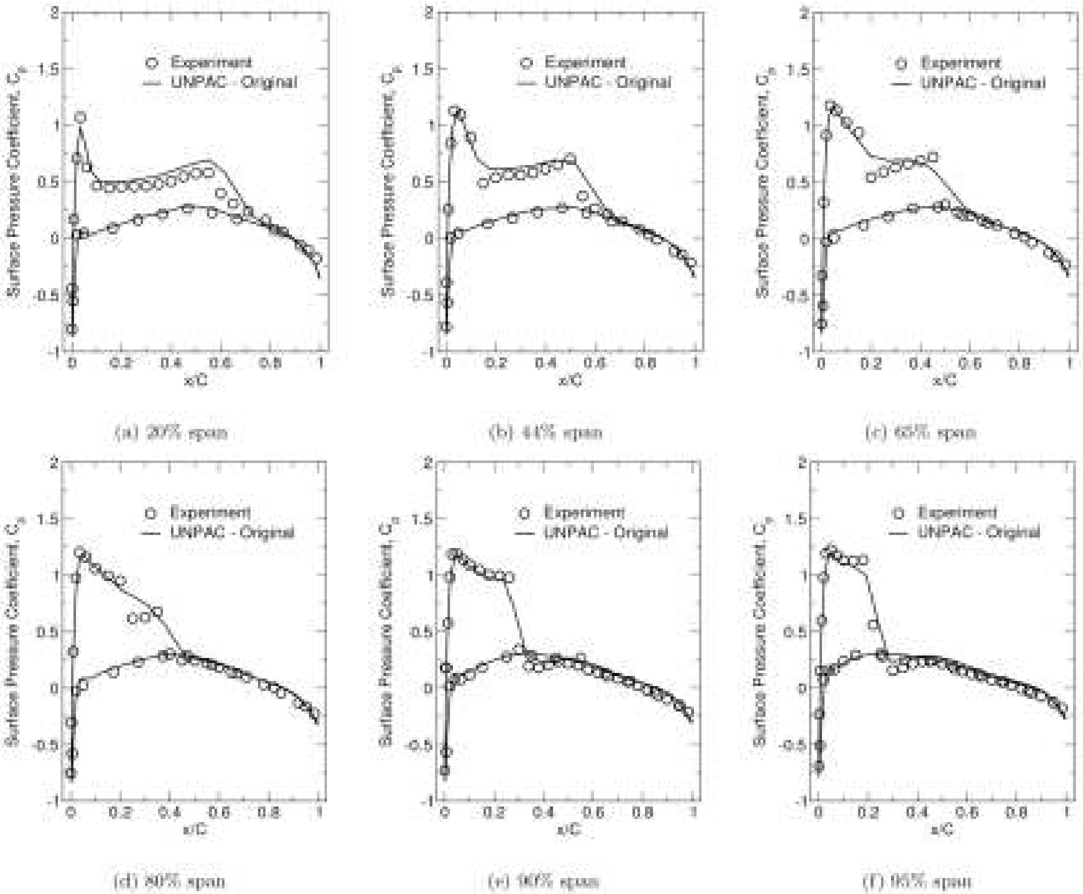

(a) 20% span (b) 44% span (c) 65% span (d) 80% span (e) 90% span (f) 95% span

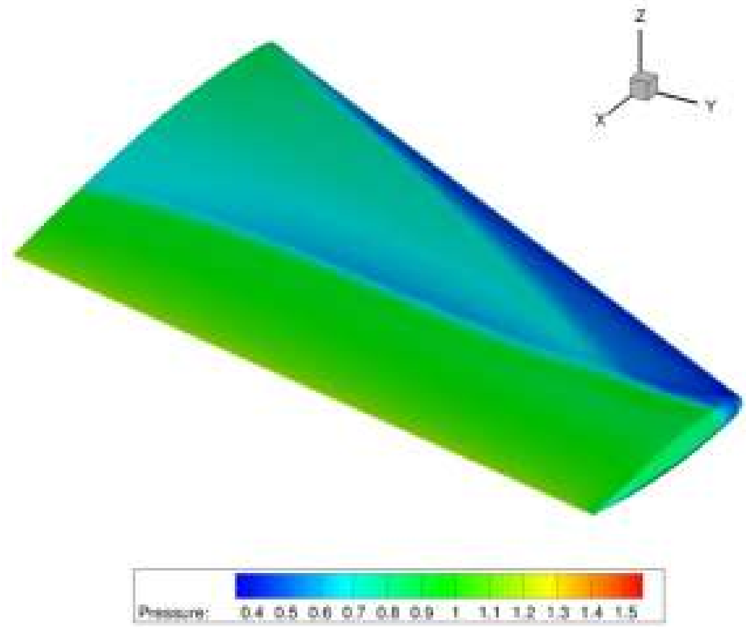

Design Optimization Results

ONERA M6 Wing

- Drag Minimization:
  - M = 0.8395, AoA = 3.06 deg

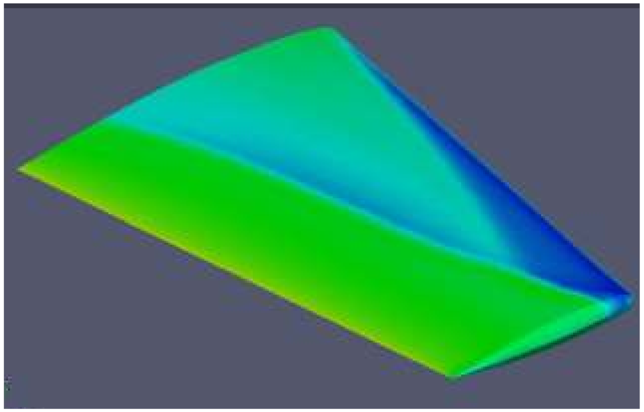

Geometry	C_D	Reduction
Original	1.1734E-2	-
Optimized	8.4601E-3	27.9%

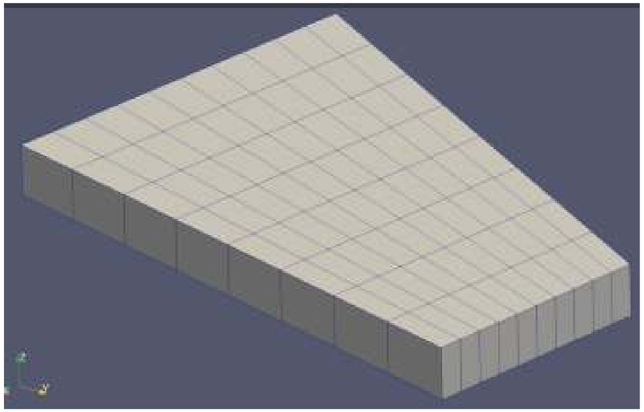

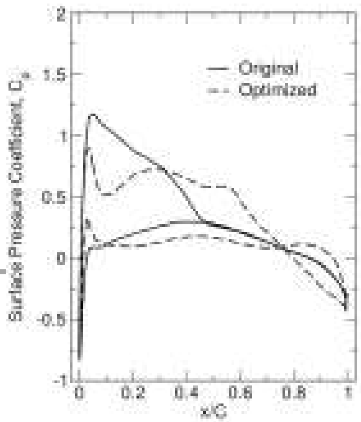

(a) 80% span

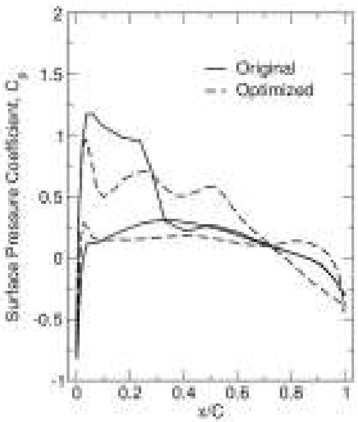

(b) 90% span

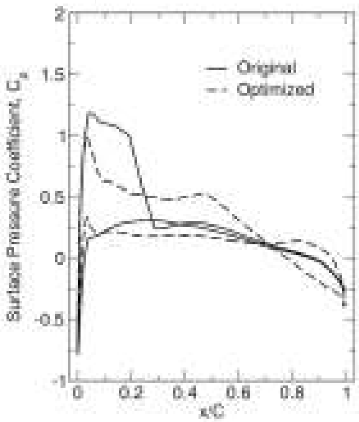

(c) 95% span

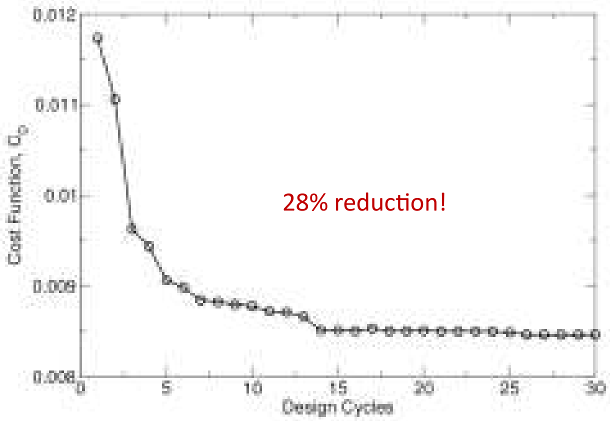

Design Optimization Results

ONERA M6 Wing

- **Drag Minimization:**
    - M = 0.8395, AoA = 3.06 deg

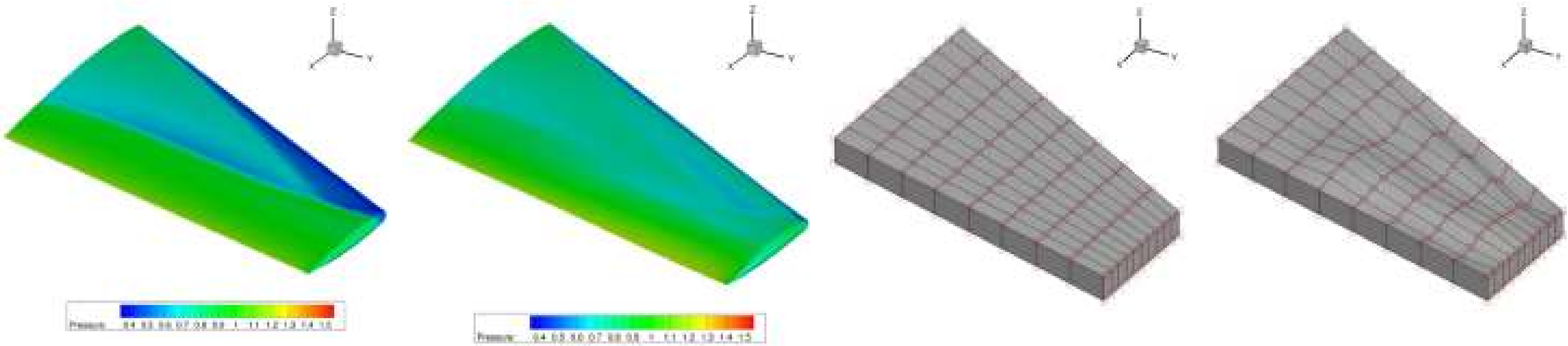

Geometry	C_D	Reduction
Original	1.1734E-2	-
Optimized	8.4601E-3	27.9%

Memory Footprint:
Adjoint Solver -> 14.1 **Gbytes**

Normalized CPU Time:

Machine Learning and Neural Networks

For Unsteady Flow Predictions

COMPUTATIONAL FLUID DYNAMICS
LABORATORY

THE UNIVERSITY OF
TENNESSEE
KNOXVILLE

Machine Learning (ML)
Artificial Neural Networks (ANN)

Artificial Intelligence Based on ML/ANN

- Multi-Layer Perceptron Network

$$\frac{\partial C}{\partial z_n} = \frac{\partial C}{\partial f(z_{n+1})}\frac{\partial f(z_{n+1})}{\partial z_{n+1}}\frac{\partial z_{n+1}}{\partial X_n}\frac{\partial X_n}{\partial z_n} = (\delta_{n+1})(w_{n+1})(f'(z_n)) = \delta_n$$

$$\frac{\partial C}{\partial w_{n+1}} = \frac{\partial C}{\partial f(z_{n+1})}\frac{\partial f(z_{n+1})}{\partial z_{n+1}}\frac{\partial z_{n+1}}{\partial w_{n+1}} = \delta_{n+1}X_n$$

$$w_{n+1} = w_n + \alpha\frac{\partial C}{\partial w_n}$$

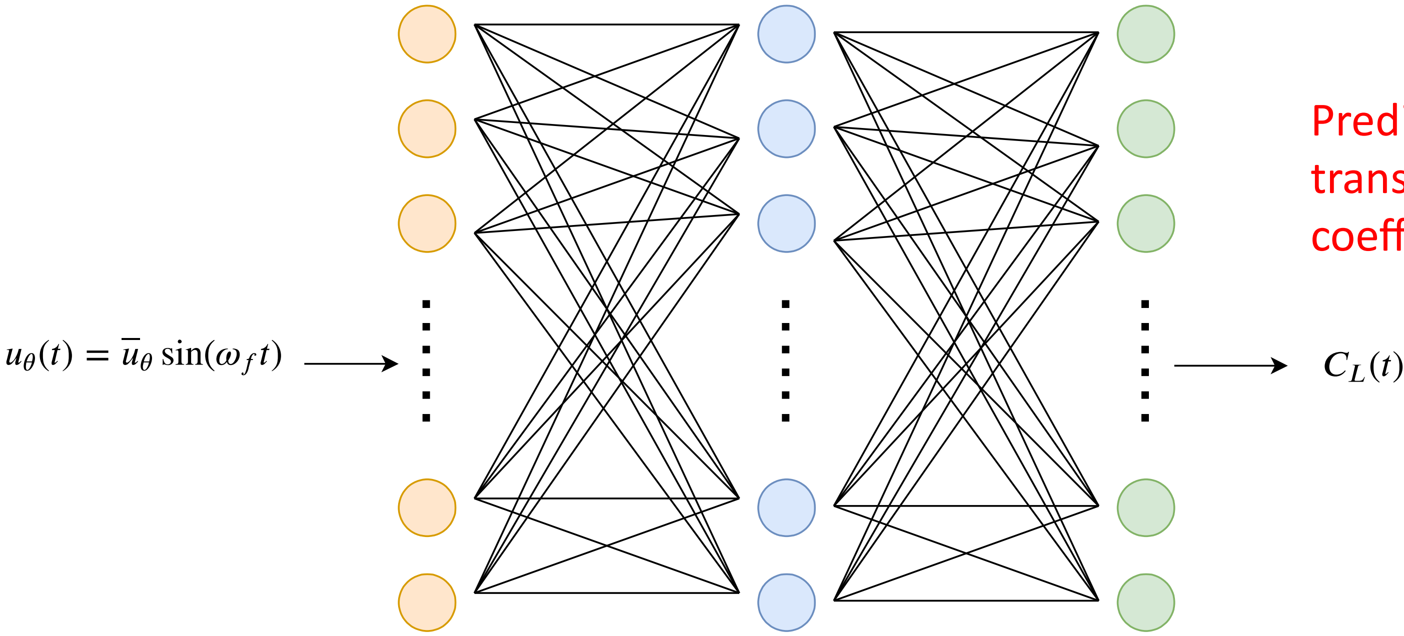

Predicting transient lift coefficient, C_L

Machine Learning (ML)
Artificial Neural Networks (ANN)

Artificial Intelligence Based on ML/ANN

- Problem Formulation:

Governing Eqn's:

$$\frac{\partial \omega}{\partial t} + J\left(\frac{\partial\psi}{\partial\eta}\frac{\partial\omega}{\partial\xi} - \frac{\partial\psi}{\partial\xi}\frac{\partial\omega}{\partial\eta}\right) = \frac{1}{R_e}\left(\alpha\frac{\partial^2\omega}{\partial\xi^2}+2\gamma\frac{\partial^2\omega}{\partial\xi\partial\eta}+\beta\frac{\partial^2\omega}{\partial\eta^2}+P\frac{\partial\omega}{\partial\xi}+Q\frac{\partial\omega}{\partial\eta}\right)$$

$$\alpha\frac{\partial^2\psi}{\partial\xi^2}+2\gamma\frac{\partial^2\psi}{\partial\xi\partial\eta}+\beta\frac{\partial^2\psi}{\partial\eta^2}+P\frac{\partial\psi}{\partial\xi}+Q\frac{\partial\psi}{\partial\eta} = -\omega$$

Rotationally oscillating cylinder in cross-flow:

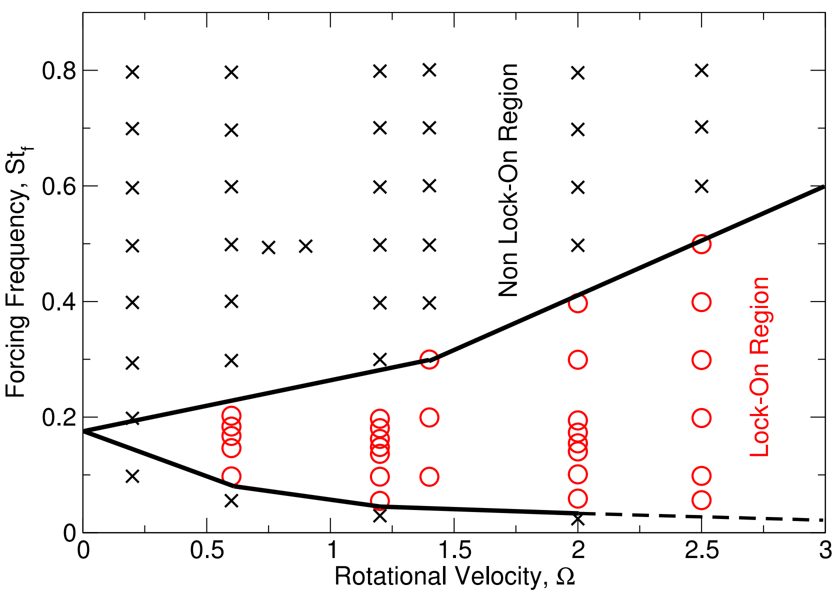

Choi et al. 2002

Machine Learning (ML) Artificial Neural Networks

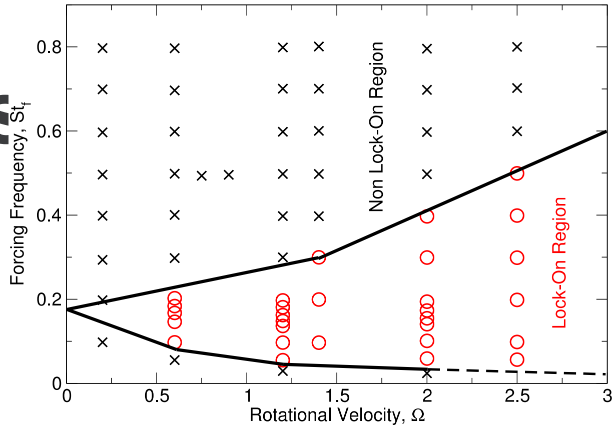

Artificial Intelligence Based on ML/ANN

➢ Flow Prediction Results:

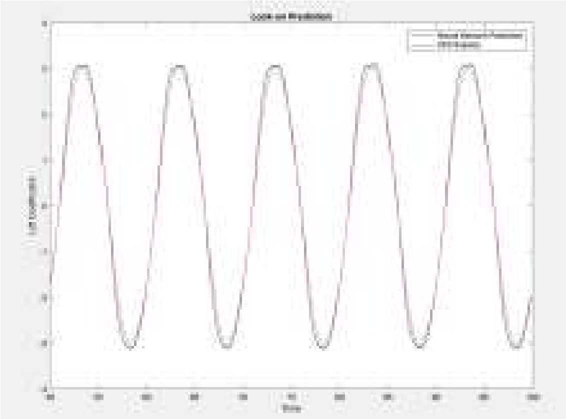

"Lock-in case"

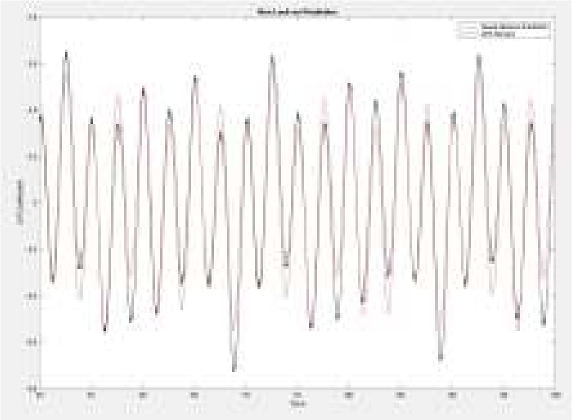

"Non-Lock-in case"

Lock-In and Non-Lock-In Regions Predicted Using ML

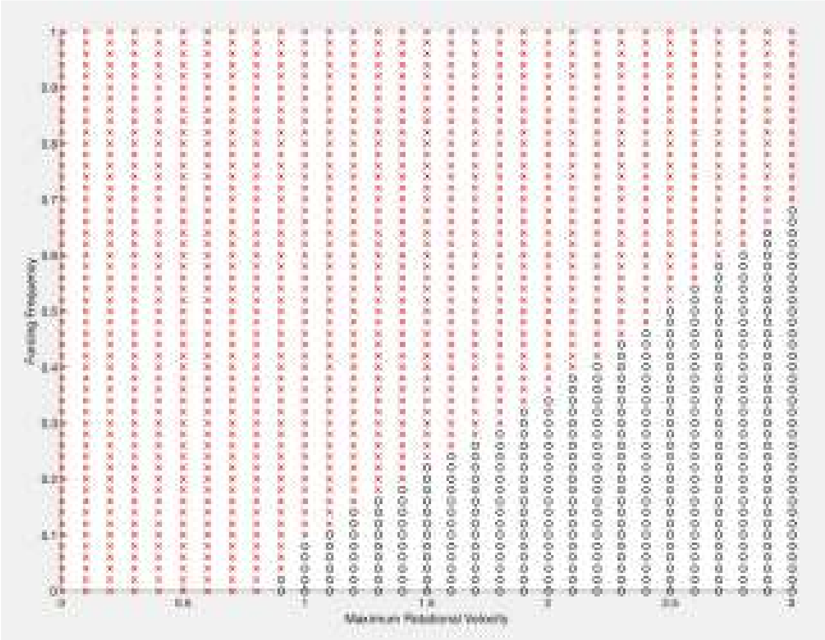

Conclusion

Summary

Future Works

COMPUTATIONAL FLUID DYNAMICS
LABORATORY

THE UNIVERSITY OF
TENNESSEE
KNOXVILLE

Summary: Computational Aeroelasticity

- **A novel dynamic aeroelastic solution approach, called the One-shot method, is developed, which features the following advantages:**

☑ **High efficiency and robustness**

Both flow and structure solvers converge simultaneously, and numerical convergence is ensured for a wide range of initial guesses

☑ **DOF-independent computational cost**

☑ **Free from time-synchronization**

Both flow and structure solvers preserve relative independence while being coupled in pseudo-time, which greatly improves the efficiency

☑ **Flexible inputs**

Prescribe either aerodynamic parameter (velocity) or structure parameter (amplitude) as the input; Capacity of resolving both benign and detrimental types of LCO, and flutter onset point using one solver

Summary: Computational Aeroelasticity

☑ **Frequency (and Velocity) search procedure**
Determine self-excited flutter and LCO;

☑ **Implicit CSD solver**
Significantly reduces the artificial energy at interface of CFD and CSD solvers, and stabilizes the coupled aeroelastic solver;

☑ **Easy implementation**
Partitioned code-coupling can be done based on off-the-shelf standalone solvers; No dynamic mesh technique is needed, and no Jacobian terms are involved;

➢ **The One-shot method has been applied to model various aeroelastic systems. Numerical results show that this new approach can rapidly predict flutter boundary and different types of LCO responses, offering a promising tool to solve dynamic aeroelasticity problems**

Future Works: Computational Aeroelasticity

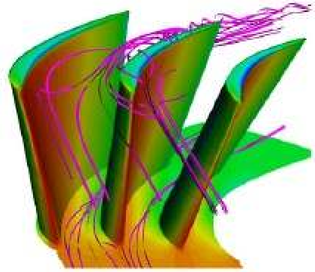

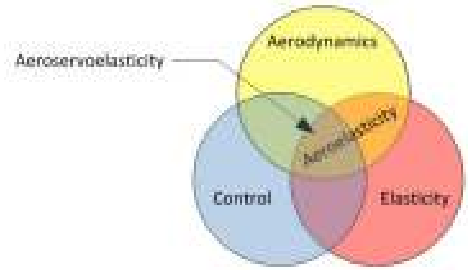

whirl flutter

turbomachinery

aeroservoelasticity

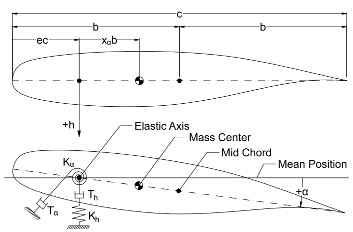

One-shot

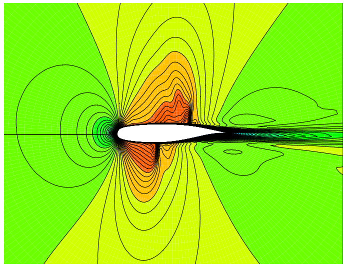

aerothermal-elasticity

“non-lock-in” vibration

Summary: Aerodynamic Design Optimization

- Grid-transparent unstructured 2D and 3D compressible RANS solver
  UNstructured **PA**rallel **C**ompressible (**UNPAC**)

- A novel toolbox for sensitivity analysis based on discrete adjoint method:
  - **F**ast automatic **D**ifferentiation using **O**perator-overloading **T**echnique (**FDOT**)
  - Efficient and fully-automated; requiring minimal changes to the primal solver
  - Memory efficient (manageable memory footprint for 2D and 3D cases)
  - Computationally efficient (Adjoint/Primal normalized CPU time **~ 2 - 5x**

UNPAC Design Optimization Framework

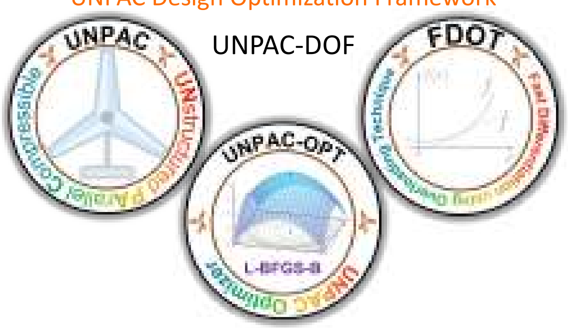

- Design Optimization Framework
  UNPAC-DOF Wrapper Program
  - Performs Gradient-Based Design Optimization
  - Uses L-BFGS-B Optimizer Program
  - Unbounded and Bound Constrained Optimization
  - Surface Points (2D) & FFD Box for Shape Parameterization/Deformation

Future Works: Aerodynamic Design Optimization

- Improving the Memory and Computational Efficiency:
  - **Optimizing the tape recording process for the expression tree**
  - Use of recursive patterns for reducing tape size ***(will require more changes to be made to the original solver)***
    - using directive functions to automize tape recording without requiring a significant amount of user intervention

- **One-Shot Method** for simultaneous solution of "**Primal**", "**Adjoint**", and "**Design**" problems

Thank You!

Q & A

THE UNIVERSITY OF
TENNESSEE
KNOXVILLE
BIG ORANGE. BIG IDEAS.®

Backup Slides

COMPUTATIONAL FLUID DYNAMICS
LABORATORY

THE UNIVERSITY OF
TENNESSEE
KNOXVILLE

Validation & Verification Results

RAE "A" Wing-Body Configuration

COMPUTATIONAL FLUID DYNAMICS
LABORATORY

THE UNIVERSITY OF
TENNESSEE
KNOXVILLE

Aeroelastic Results

1-DOF Vortex Induced Vibration (VIV)

- **Sweep over *Reynolds number***

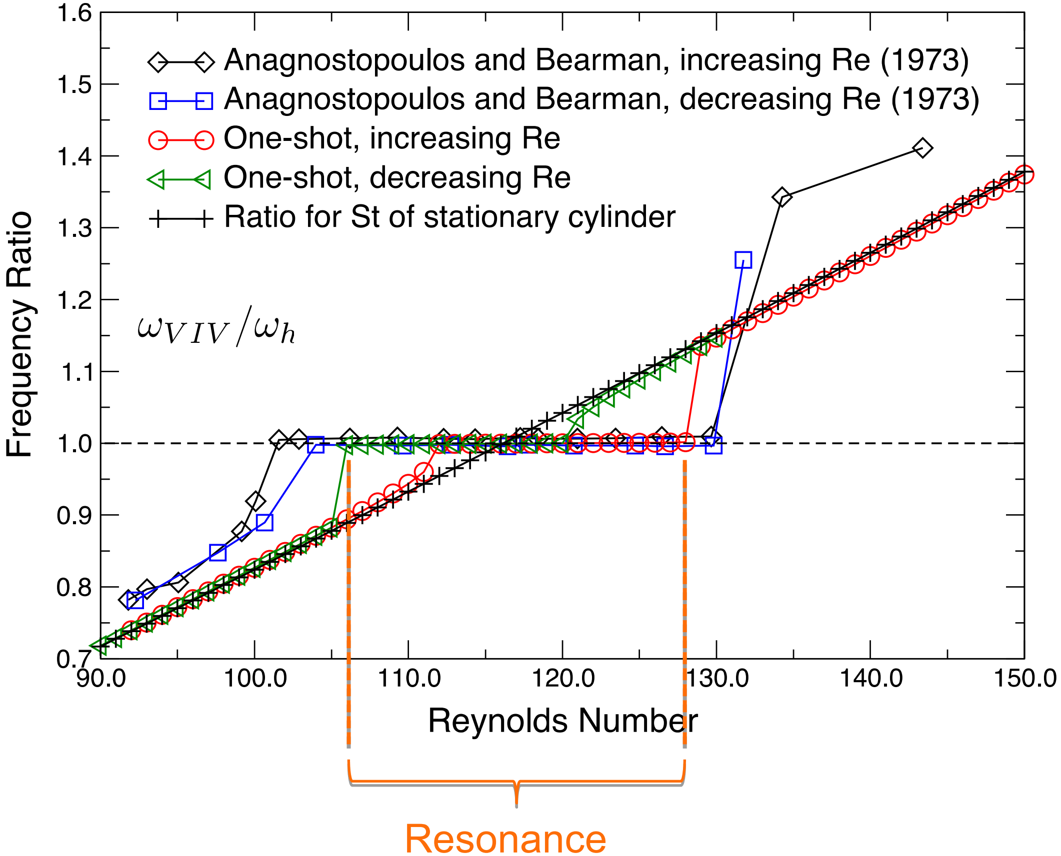

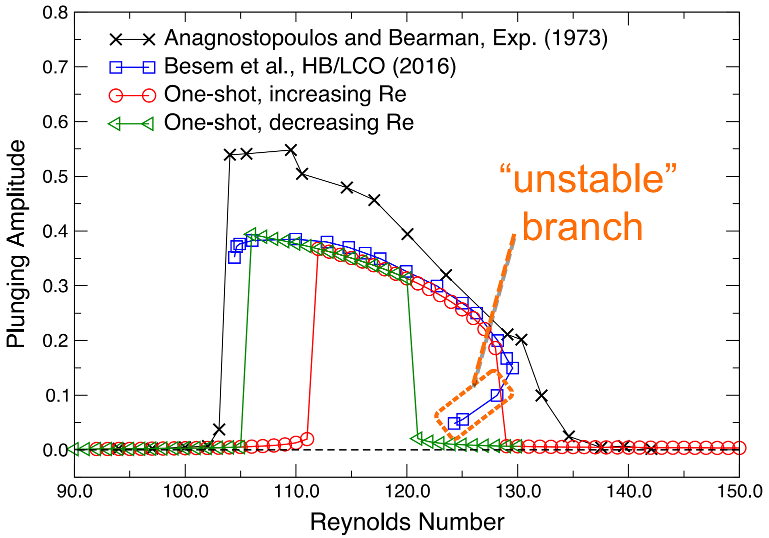

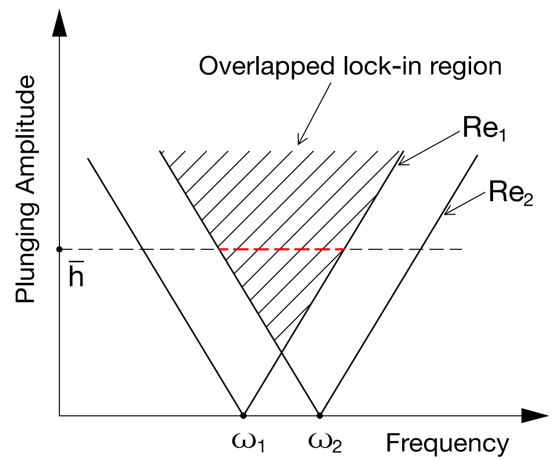

"Lock-in" of three frequencies: $\omega_{VIV}, \quad \omega_{vortex}, \quad \omega_h$

Validation & Verification Results

RAE “A” Wing-Body Configuration (AGARD-AR-138, Case 6)

- M = 0.9, AoA = 1.0 deg
- RAE “A” Wing:
  - A.R. = 5.5
  - L.E. Sweep Angle = 36.7 deg
  - T.E. Sweep Angle = 22.3 deg
  - Taper ratio = 0.375
  - RAE 101 symmetrical airfoils (untwisted)
- Unstructured Grid, ~460K tetrahedra, exte

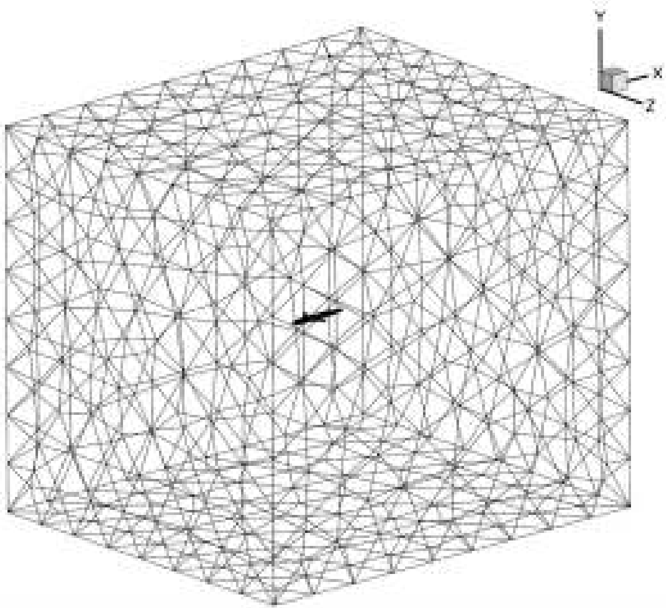

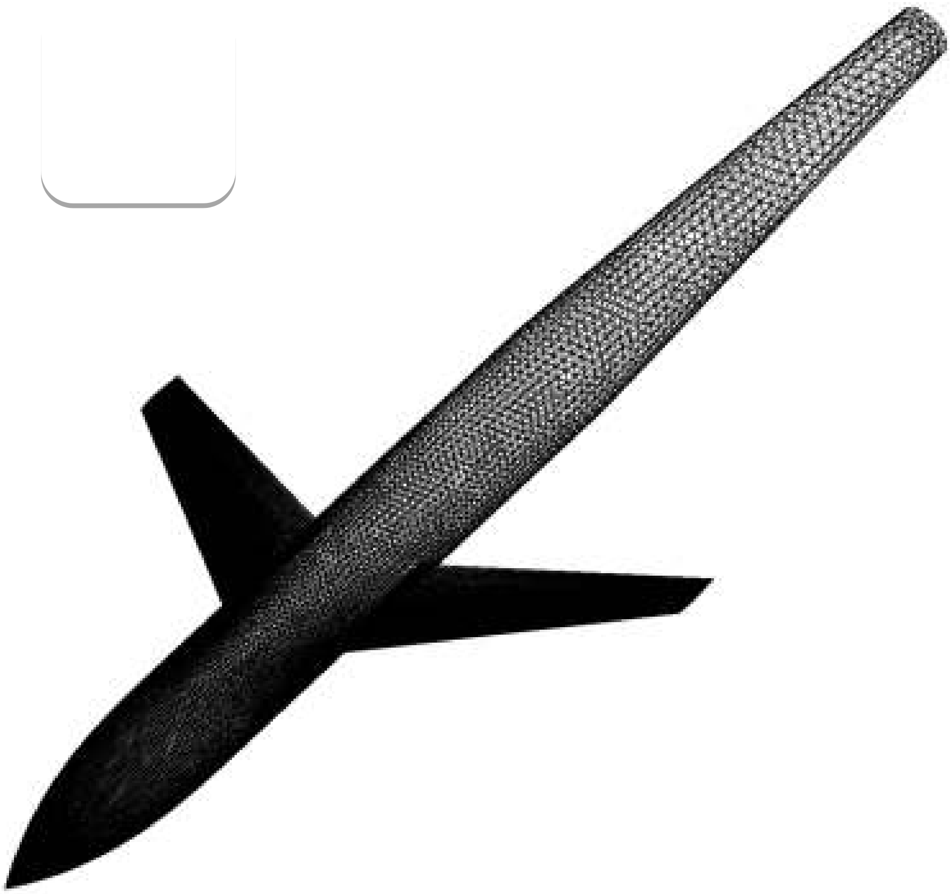

Validation & Verification Results

RAE “A” Wing-Body Configuration (AGARD-AR-138, Case 6)

- Mach number and Pressure Contours

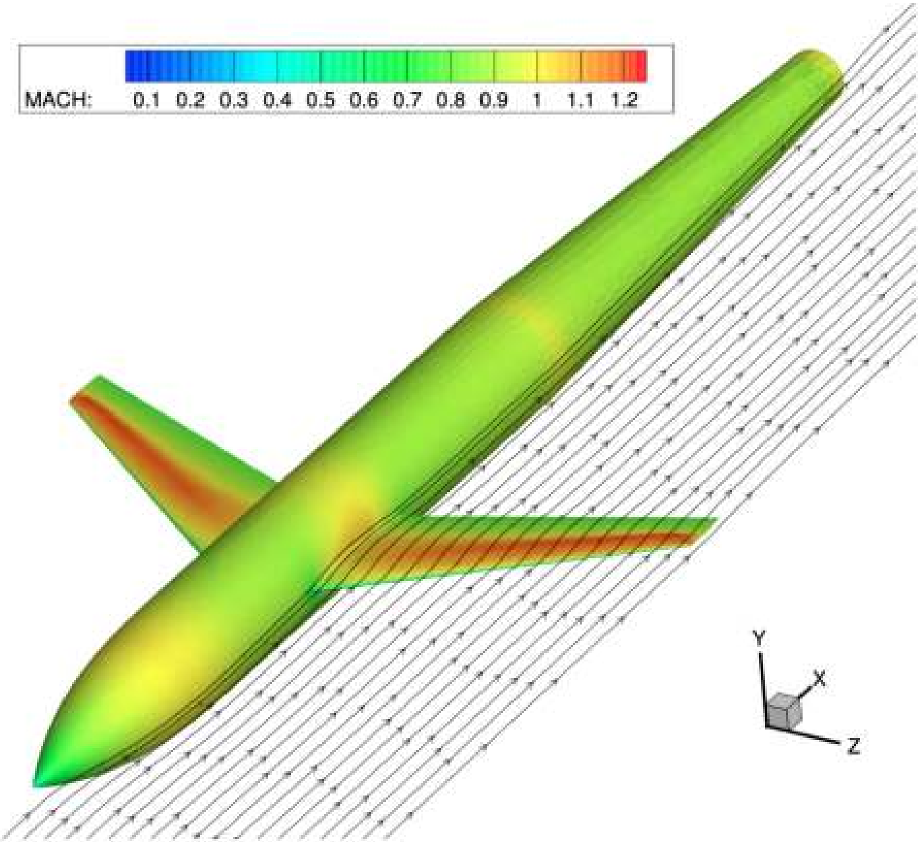

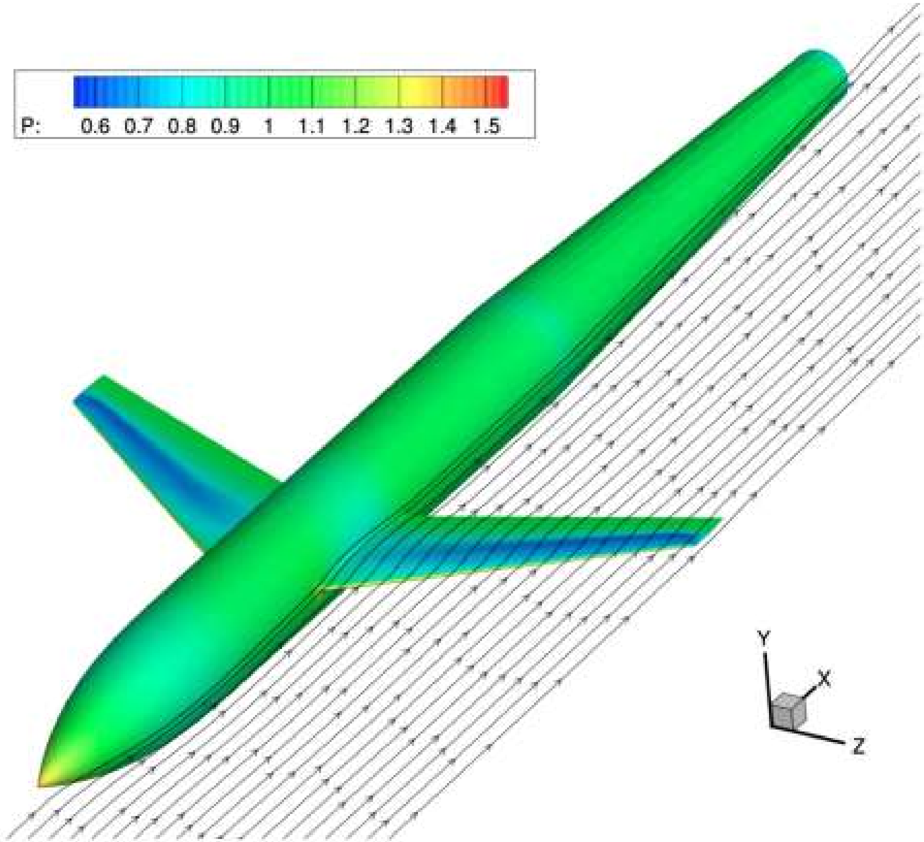

Validation & Verification Results

RAE "A" Wing-Body Configuration (AGARD-AR-138, Case 6)

- Pressure Coefficients at Various Spanwise Location Along the Wing

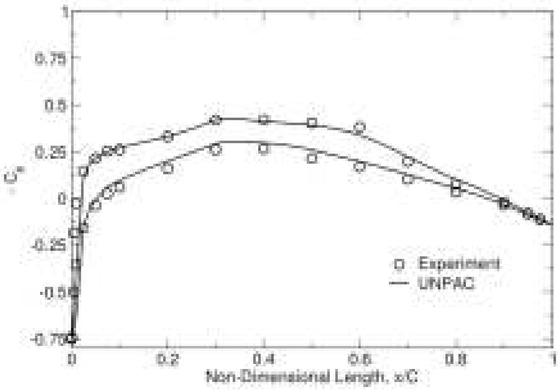

(a) 25% span

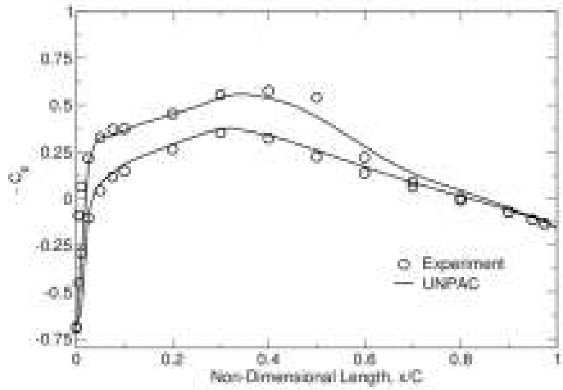

(b) 40% span

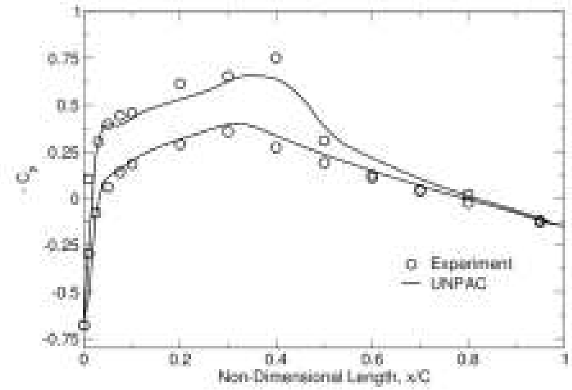

(c) 60% span

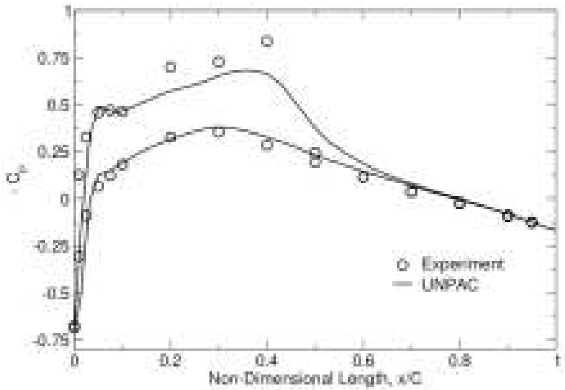

(d) 75% span

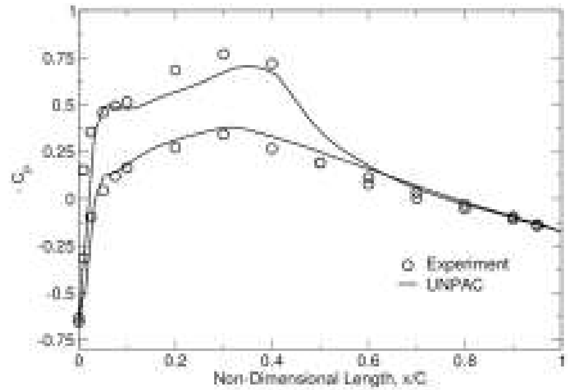

(e) 85% span

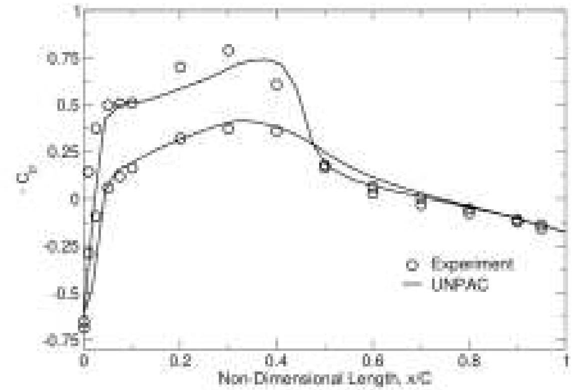

(f) 92.5% span

Validation & Verification Results

RAE "A" Wing-Body Configuration (AGARD-AR-138, Case 6)

➢ Pressure Coefficients Distributions for 2 Longitudinal Sections along the body

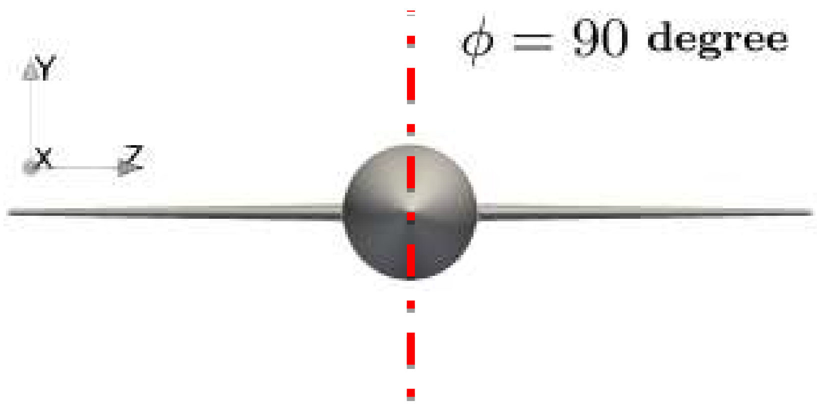

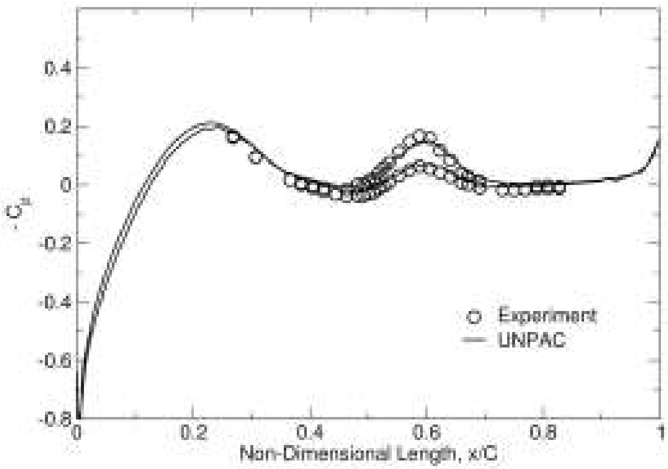

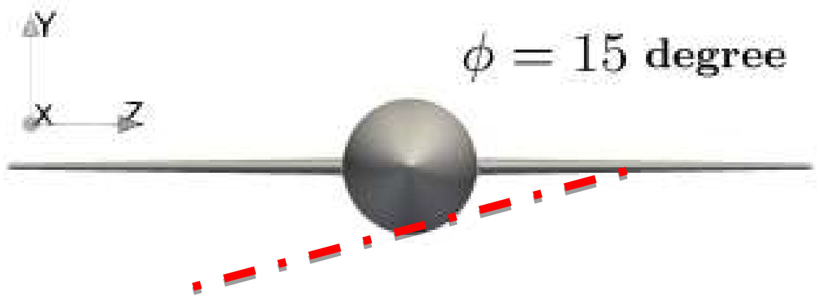

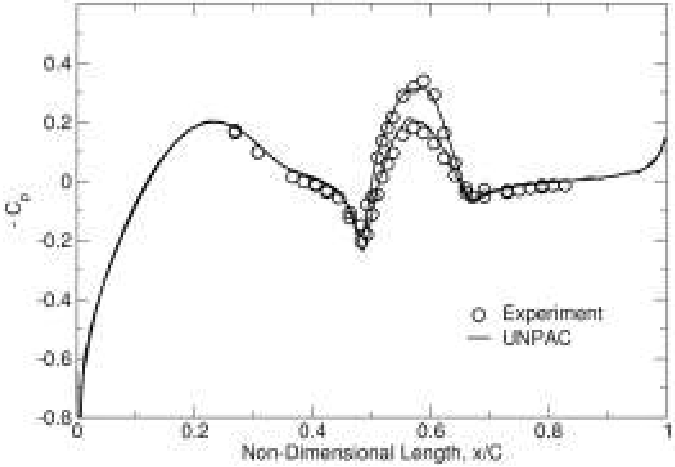

THE UNIVERSITY OF TENNESSEE KNOXVILLE

ROM-Based Convergence Acceleration

COMPUTATIONAL FLUID DYNAMICS
LABORATORY

THE UNIVERSITY OF
TENNESSEE
KNOXVILLE

ROM-Based Convergence Acceleration

ROM-Based Convergence Acceleration

- Model Reduction: $\frac{d\vec{U}}{dt} + \mathcal{N}(\vec{U}) = 0$ ROM $\Phi^T \frac{d}{dt}\left(\Phi\vec{\xi}\right) + \Phi^T\mathcal{N}\left(\Phi\vec{\xi}\right) = 0$ where $\vec{U} \cong \Phi\vec{\xi}$

- Update formula: $\vec{U}^{n+1} = \vec{U}^n + \vec{R}(\vec{U})$

$$\boxed{\vec{R}(\vec{U}) \approx \mathbf{A}\vec{U} - \vec{b}}$$

Assumption

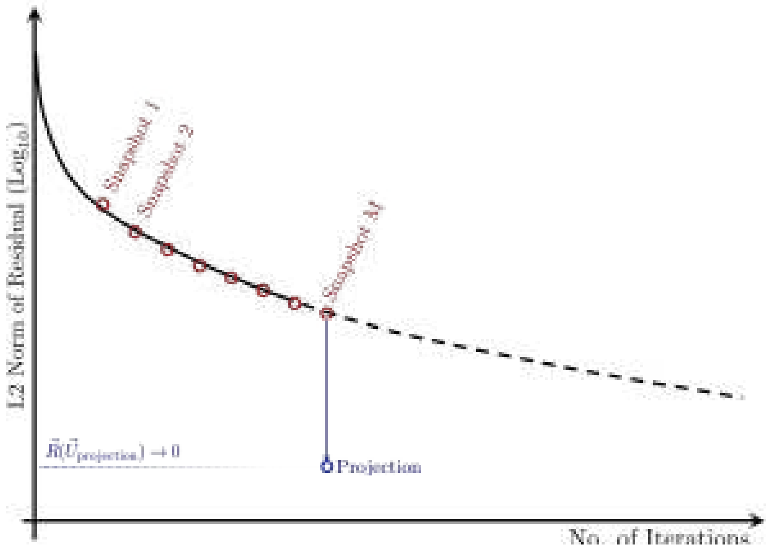

Correlation-Based Approach

$$\Phi = \begin{bmatrix} | & | & & | \\ \vec{U}_1 & \vec{U}_2 & \dots & \vec{U}_M \\ | & | & & | \end{bmatrix}_{N\times M} \qquad \vec{U}_{\text{projected}} = \sum_{i=1}^{M} \vec{U}_i \xi_i = \mathbf{\Phi}\,\boldsymbol{\xi}$$

Covariance-Based Approach

$$\hat{\Phi} = \begin{bmatrix} | & | & & | \\ \vec{U}_1 - \overline{\vec{U}} & \vec{U}_2 - \overline{\vec{U}} & \dots & \vec{U}_M - \overline{\vec{U}} \\ | & | & & | \end{bmatrix}_{N\times M} \qquad \vec{U}_{\text{projected}} = \hat{\mathbf{\Phi}}\,\vec{\xi} + \overline{\vec{U}} \qquad \overline{\vec{U}} = \frac{1}{M}\sum_{i=1}^{M}\vec{U}_i$$

ROM-Based Convergence Acceleration

Inviscid Transonic Flow Past NACA0012 Airfoil

- ROM-Based Convergence Acceleration:
  - Covariance-based approach
  - 10, 20, 40, and 80 solution snapshots used for projections (over a span of 2000 iterations)
  - Process lagged by 1000 iterations (2 orders of magnitude drop in residual)

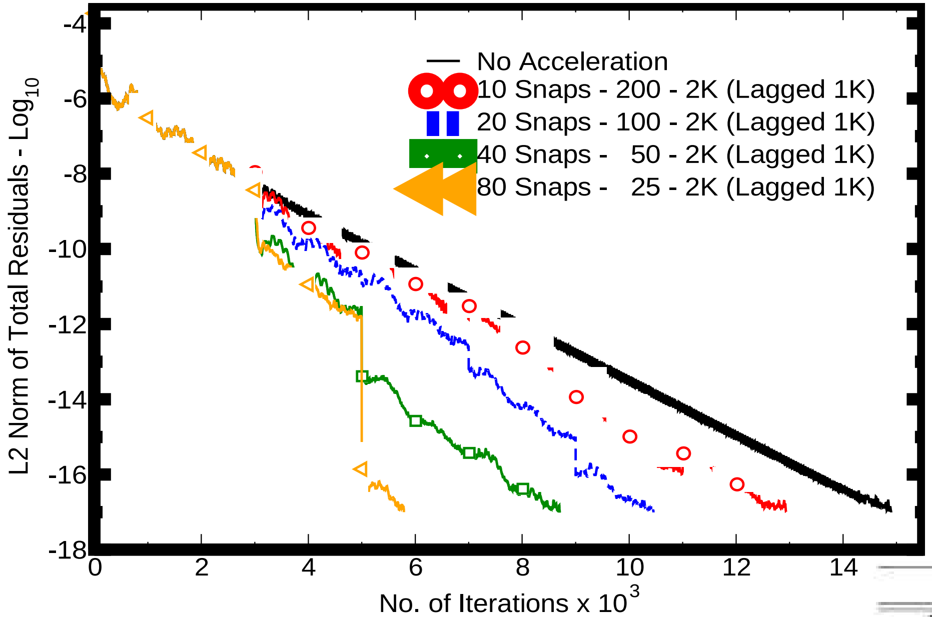

Case Settings

$$M_\infty = 0.8$$
$$\alpha = 1.25 \text{ deg}$$

Reductions in Iterations and CPU Time

Test	Iterations	Reduction	CPU time (s)	Reduction
No Acceleration	14,899	-	215.58	-
10 - 200 - 2K (L-1K)[a]	12,930	13.21%	188.09	12.75%
20 - 100 - 2K (L-1K)	10,451	29.86%	154.64	28.27%
40 - 50 - 2K (L-1K)	8,699	41.61%	131.59	38.96%
80 - 25 - 2K (L-1K)	5,788	61.15%	93.28	56.73%

[a] 10 snapshots every 200 iterations during a cycle of 2,000 itrs. and lagged by 1,000 itrs.

Adaptive Mesh Redistribution (AMR)

COMPUTATIONAL FLUID DYNAMICS
LABORATORY

THE UNIVERSITY OF
TENNESSEE
KNOXVILLE

Adaptive Mesh Redistribution (AMR)

r-Adaptive Mesh Redistribution (AMR)

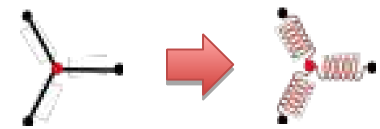

- Ball-Vertex Approach (Spring Analogy):
  - Node relocation to have clustering around regions of large flow gradients $\vec{F}_i = K_i \vec{\Delta x}_i$
  - Hook's law:

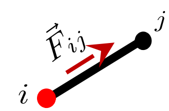

Force field: combination of gradient & curvature forces acting on the two end nodes

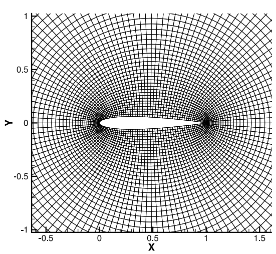

Baseline Grid

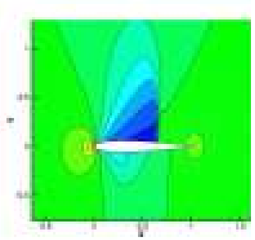

Solution Field

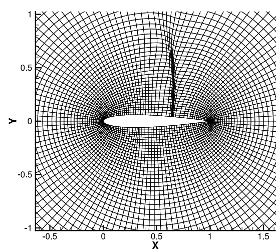

Adapted Grid

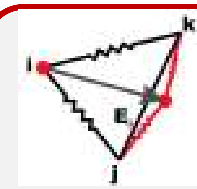

Mesh Entanglement

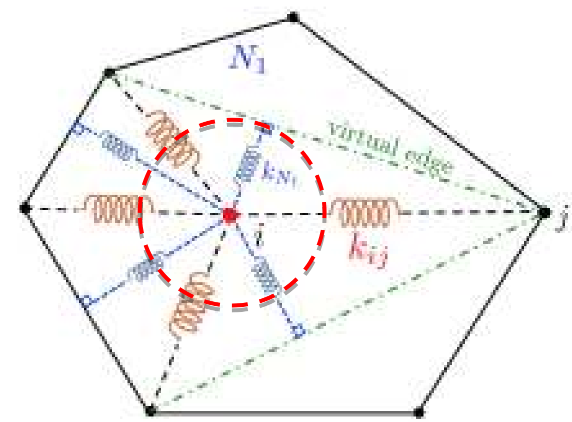

- **Local relaxation:**

$$\vec{x}_i^{\,new} = \vec{x}_i^{\,old} + \omega_i \, \vec{\Delta x}_i$$

where $\omega_i = \begin{cases} \dfrac{\lambda \, L_{i,\,min}}{\|\vec{\Delta x}_i\|} & \text{if} \quad \|\vec{\Delta x}_i\| > \lambda L_{i,\,min} \\ 1 & \text{otherwise} \end{cases}$

- **Boundary Correction:**

$$\vec{x}_i^{\,\text{bndy correction}} = \vec{x}_i - \left(\vec{x}_i \cdot \vec{S}_n\right) \vec{S}_n$$

Adaptive Mesh Redistribution (AMR)

Inviscid Transonic Flow Past NACA0012 Airfoil

- r-Adaptive Mesh Redistribution (AMR):
  - Convergence and Errors

Case Settings

$$M_\infty = 0.8$$
$$\alpha = 1.25 \text{ deg}$$

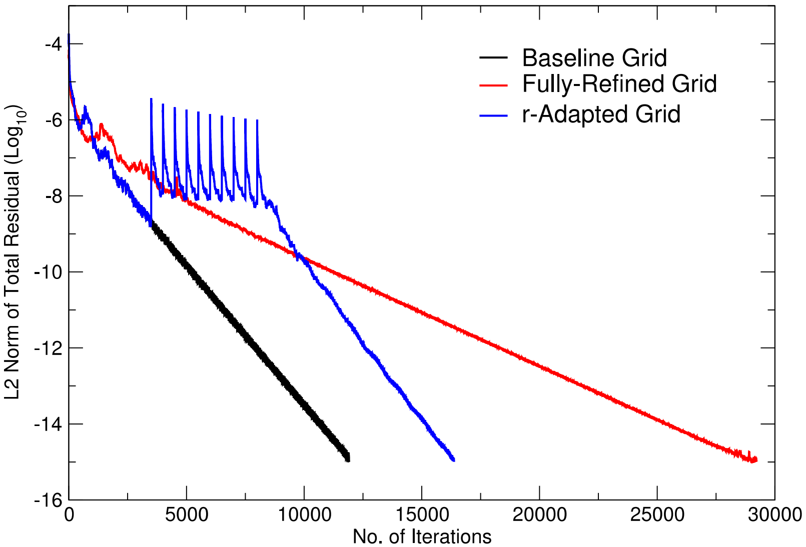

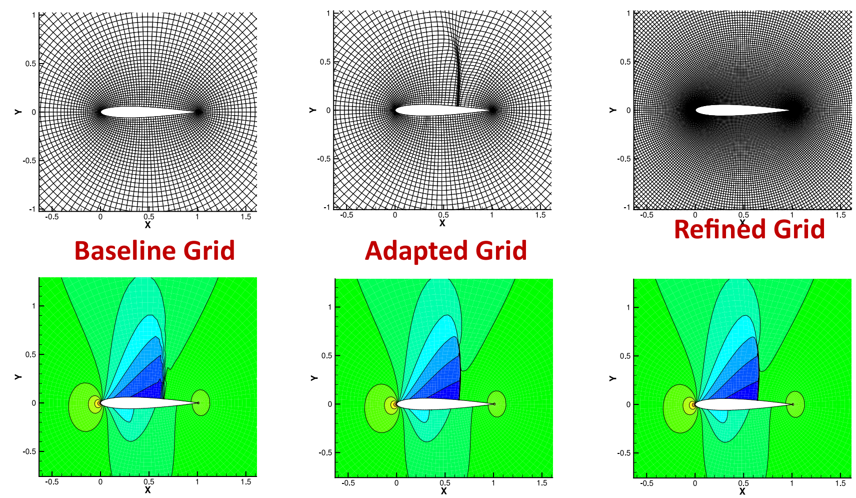

Lift and Drag Predictions

Grid	C_L	Error	Error (relative)	C_D	Error	Error (rel.)
Yano & Darmofal [217]	0.35169	-	-	0.02262	-	-
Fully-Refined	0.35096	0.20%	-	0.02349	3.84%	-
Baseline	0.34820	0.99%	1.64%	0.02445	8.09%	4.08%
r-adapted (AMR)	0.35024	0.41%	0.20%	0.02302	1.76%	2.00%

Computational Cost

Grid	CPU Time (s)	Normalized CPU Time
Baseline	215.58	1.00
Fully-Refined	2037.60	9.45
r-adapted (AMR)	**306.27**	**1.42**

Adaptive Mesh Redistribution (AMR)

AGARD-702 CT5 Case

- Inviscid Periodic Flow:
  - Unstructured Grid:
    Nodes = 5,233
    Cells = 10,216
  - Harmonic Balance Method

Case Settings

$$M_\infty = 0.755$$
$$\alpha_0 = 0.016 \text{ deg}$$
$$\alpha_p = 2.51 \text{ deg}$$
$$k = 0.0814$$

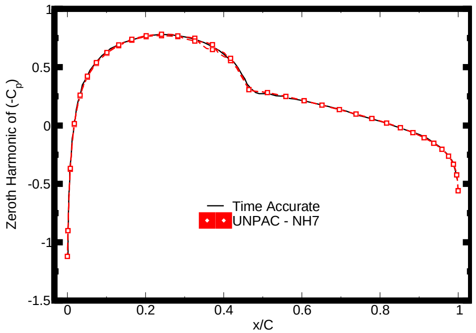

Zeroth Harmonic of Surface Pressure

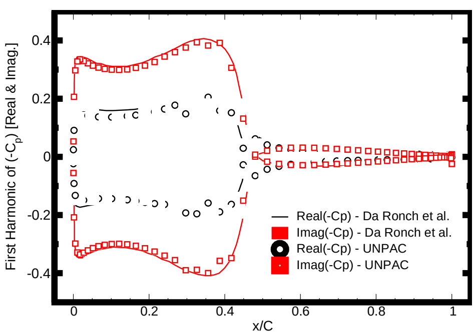

First Harmonic of Surface Pressure

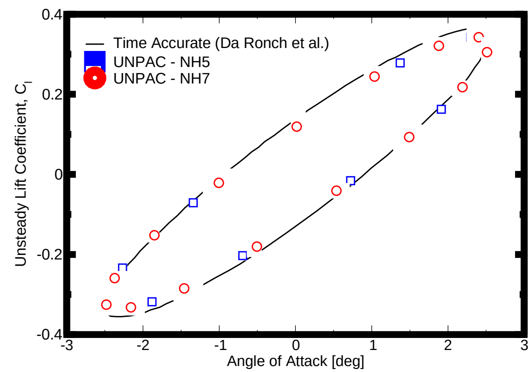

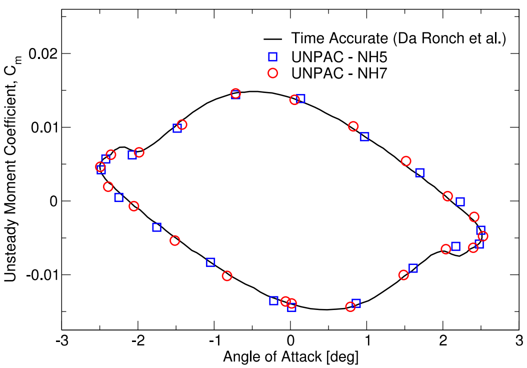

Mesh Motion

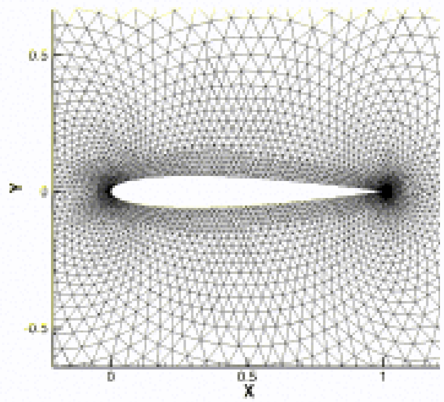

Unsteady Mach number contours

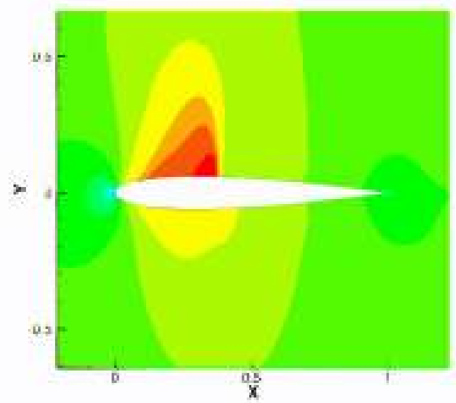

Sine Motion about 25%-chord pitching axis

Adaptive Mesh Redistribution (AMR)

AGARD-702 CT5 Case

- r-Adaptive Mesh Redistribution (AMR):
  - Baseline grid:
    Nodes = 1,837
    Cells = 3,542
  - Fully-refined grid:
    Nodes = 5,233
    Cells = 10,216

Case Settings

$$M_\infty = 0.755$$
$$\alpha_0 = 0.016 \text{ deg}$$
$$\alpha_p = 2.51 \text{ deg}$$
$$k = 0.0814$$

Baseline Grid

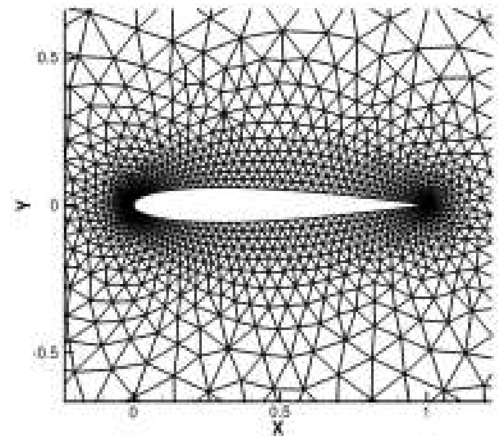

Fully-refined Grid

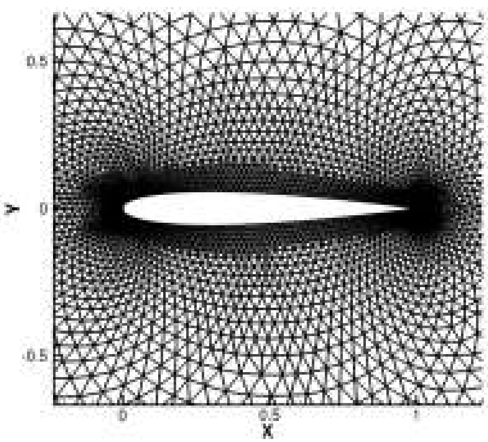

r-Adapted Grid at various sub-time levels

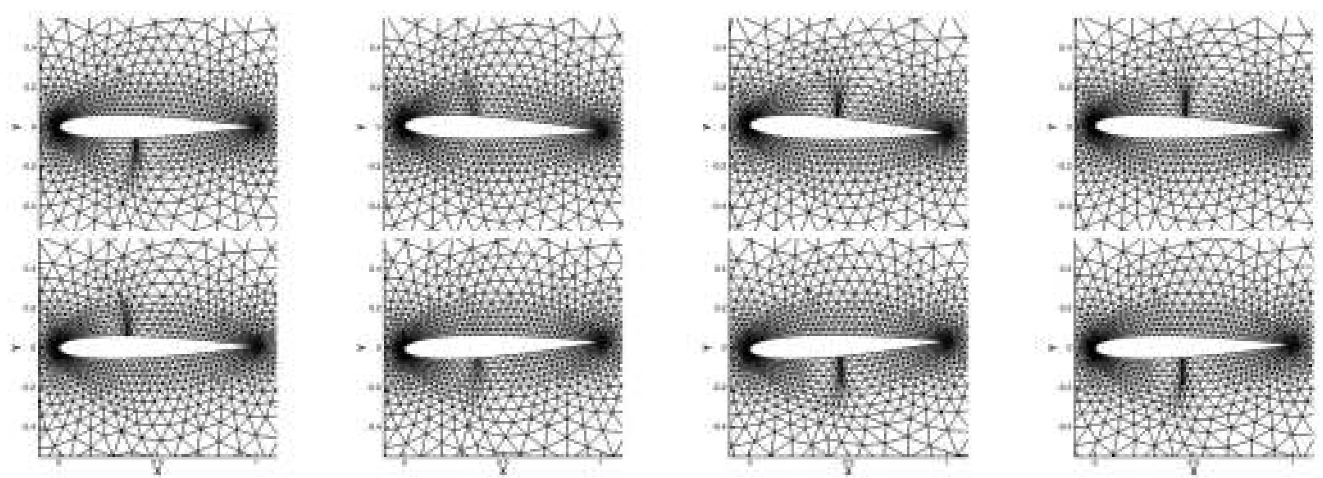

Adaptive Mesh Redistribution (AMR)

AGARD-702 CT5 Case

- r-Adaptive Mesh Redistribution (AMR):
  - Significant improvements in numerical accuracy at a fraction of the computational cost

Case Settings

$$M_\infty = 0.755$$
$$\alpha_0 = 0.016 \text{ deg}$$
$$\alpha_p = 2.51 \text{ deg}$$
$$k = 0.0814$$

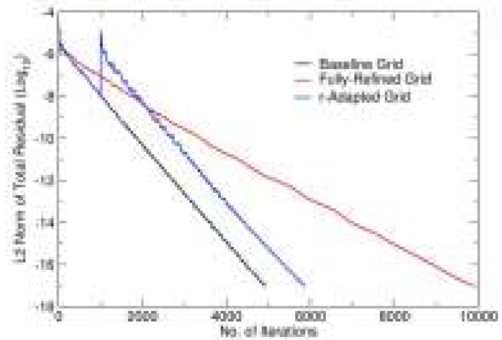

L2 Norm of Errors in C_L and C_M

Coefficient	Baseline Grid	r-Adapted Grid
C_l	-2.878065	**-5.792785**
C_m	-1.992387	**-5.063434**

Computational Cost Comparison

Grid	CPU Time (s)	Normalized CPU Time
Baseline	1,749.1	1.00
Fully-Refined	12,671.2	7.24
r-adapted (AMR)	**2,207.2**	**1.26**